Chemical Engineering Journal Advances 6 (2021) 100091

Contents lists available at ScienceDirect

Chemical Engineering Journal Advances

journal homepage: www.elsevier.com/locate/ceja

Review

A review on recent advances in CO_2 separation using zeolite and zeolite-like materials as adsorbents and fillers in mixed matrix membranes (MMMs)

Moustafa M. Zagho[a,*], Mohammad K. Hassan[b,*], Majeda Khraisheh[c], Mariam Al Ali Al-Maadeed[b,d], Sergei Nazarenko[a,*]

[a] School of Polymer Science and Engineering, University of Southern Mississippi, Hattiesburg, MS 39406, USA
[b] Center for Advanced Materials, Qatar University, Doha 2713, Qatar
[c] Department of Chemical Engineering, College of Engineering, Qatar University, Doha 2713, Qatar
[d] Materials Science & Technology Program (MATS), College of Arts & Sciences, Qatar University, Doha 2713, Qatar

ARTICLE INFO

Keywords:
CO_2 separation
Zeolite
Nanoparticles
Nanofibers
Zeolite-based foams
Adsorption
Mixed matrix membranes (MMMs)
Hollow zeolite spheres (HZSs)
Sheet-like particles
Zeolitic imidazolate frameworks (ZIFs)

ABSTRACT

Anthropogenic emissions have developed the environmental demands for proficient carbon dioxide (CO_2) separation technologies. Adsorption and membrane technologies are widely used to separate CO_2 from other light gases due to their multiple technological benefits, including but not limited to factors such as energy efficiency and low environmental footprint. In this context, zeolites are often used due to their intrinsic molecular sieving capacity. This review initially addresses recent technological advances to enhance the gas separation performance of zeolite materials. Current trends directed toward improving CO_2 adsorption capacity of zeolites include amine, silica, and ion-exchange modifications. Other promising efforts to improve the adsorption performance of zeolites involve processing zeolite nanoparticles, nanofibers, and zeolite-based foams. The second part of the review deals with pristine and modified zeolites beneficial properties for designing polymer-based mixed matrix membranes (MMMs), which enable to adapt a desirable gas separation performance. The gas transport mechanisms and morphological properties of MMMs are essential. This review addresses the most current strategies used to improve interfacial adhesions between zeolite particulates and polymer matrices to overcome the trade-off between gas selectivity and permeability faced by pure polymeric membranes. Filler shape and size play vital roles in determining the filler and polymer matrix's interfacial adhesions. New structures of inorganic fillers have been designed to fabricate MMMs with excellent gas transport properties. Hollow zeolite spheres (HZSs) are particularly interesting as they effectively minimize agglomeration and improve filler dispersion in the polymer matrix. Furthermore, approaches that employ nanoporous layered fillers, including AMH-3 and Jilin-Davy-Faraday, layered solid No. 1 (JDF-L1), have been reviewed to overcome the limitation of incorporating high contents of zeolites, which are required to improve the gas transport properties of MMMs. Furthermore, this review explores implementing zeolitic imidazolate frameworks (ZIFs) in MMMs because of their tunable pore structure and remarkably high adsorption capacity and surface area as well as excellent chemical and thermal properties. Lastly, we address the prospects and future developments in gas separation applications.

1. Introduction

Zeolites are natural and synthetic aluminosilicates characterized by a microporous crystal structure [1]. In natural zeolites, balancing cations are sited in relatively large cavities created by the $[Si_{1-x}Al_xO_2]^{x-}$ negatively charged frameworks [1]. These cavities are linked together by channels that generate the microporous structure, which can be penetrated by adequately small molecules, thus displaying the molecular sieving phenomena essential for separation technologies [2]. The zeolite framework is built on two key structural units constituted by aluminum or silicon atoms bonded to four oxygen atoms producing a tetrahedral shape, and an oxygen atom being attached to two tetrahedral atoms (normally bent ~ 145°) [1]. Tetrahedra are then connected, forming rings commonly comprised of 4, 5, 6, 8, 10, or 12 tetrahedra. The combination of rings forms more complex composite building units like molecular cages; the periodic arrangement of these complex units forms the framework with cavities consisting of channels, pockets, and cages,

* Corresponding authors.
E-mail addresses: moustafa.zagho@usm.edu (M.M. Zagho), mohamed.hassan@qu.edu.qa (M.K. Hassan), sergei.nazarenko@usm.edu (S. Nazarenko).

https://doi.org/10.1016/j.ceja.2021.100091
Received 17 November 2020; Received in revised form 9 January 2021; Accepted 11 January 2021

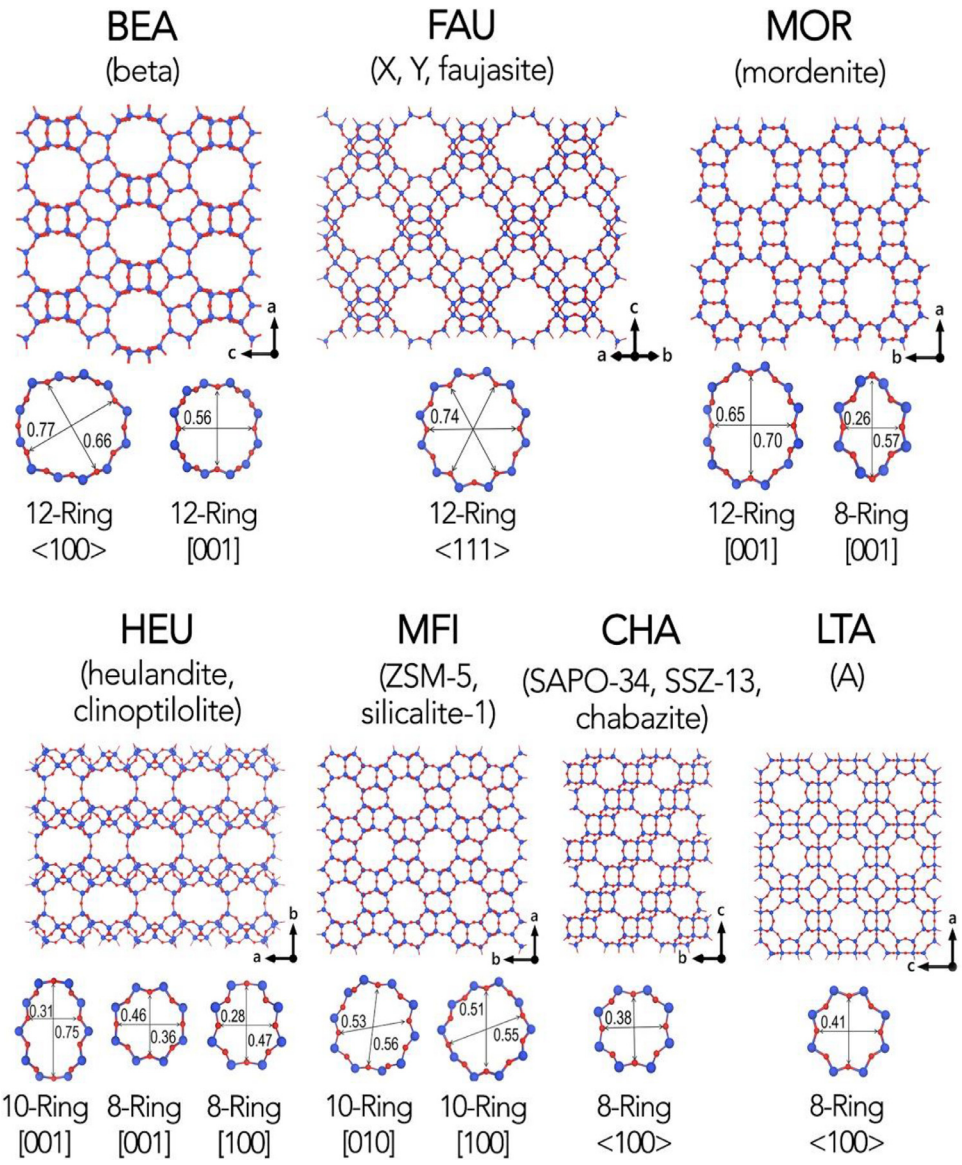

Fig. 1. Selected broadly applied zeolite frameworks. The three-letter code assigned by the International Zeolite Association (IZA) (in bold), the name of zeolites relating to the corresponding framework type, the pore window, the ball-stick atomic model, pore directions, and the ring size (in nm) are provided. Red spheres denote oxygen atoms, while blue spheres represent T atoms [24]. (For interpretation of the references to color in this figure legend, the reader is referred to the web version of this article.)

linked by rings that act as windows between the cavities. Fig. 1 demonstrates some widely used framework types.

Zeolites can be distinguished according to different standards [3], with pore aperture being of greatest interest. Zeolites can be classified as [1]: (i) small-pore zeolites, comprised of channels delimited by 8 membered rings with a pore diameter of ~ 4 Å, (ii) medium-pore zeolites, comprised of channels delimited by 10 membered rings with a pore diameter of ~ 5–6 Å, (iii) large-pore zeolites, comprised of channels delimited by 12 membered rings with a pore diameter of ~ 7 Å, and (iv) extra-large pore zeolites, comprised of channels delimited by more than 12 membered rings and a pore diameter larger than 7 Å. This is a rough classification as pore shape represents another significant criterion, wherein zeolites with pore apertures of varied shapes but delimited by the same number of tetrahedra exhibit quite different behavior. The dimensionality of the channels demonstrates another zeolite criterion, as zeolitic materials may include one-dimensional, two-dimensional, and three-dimensional pore structures, depending on channel arrangement. Moreover, zeolitic materials have also been classified as low silica (Si/Al atomic ratio ~ 1), intermediate silica (1.5 < Si/Al atomic ratio < 10), or high silica (Si/Al atomic ratio > 10). Low-silica zeolites are hydrophilic due to the high contents of protons and highly negatively charged frameworks. In contrast, high-silica zeolitic materials are hydrophobic because of the presence of predominated covalent Si-O-Si bridges. For clarifying, zeolite NaA offers excellent CO_2-over-N_2 selectivity compared to FAU due to its narrow pore window [4]. Many large-pore zeolites with channels formed by openings of more than 12 rings are known, but all of them have a one-dimensional channels that limits their use in catalysis applications [5]. Regarding the Si/Al ratio, zeolite LTA4A is commonly used to separate polar from non-polar molecules by permeation, as this zeolite is highly hydrophilic due to its low Si/Al ratio [6].

Zeolites and other molecular sieves are used for many purposes, including adsorption, membranes, ion-exchange, and catalysis, due to their high surface area, hydrothermal stability, and structure selective characteristics [7,8]. Their applications depend mainly on framework composition (Si/Al ratio and the associated hydrophilicity/hydrophobicity) and crystalline morphologies (8-, 10-, 12-ring, or larger pores and one-, two-, or three-dimensional channels) [9]. The preparation procedure represents a vital role in tailoring and applying zeolites for specific uses [9]. Principally, direct preparation and post-synthetic functionalization are commonly used to attain desired properties. In the direct preparation, the primary approach of synthesizing zeolites [10,11,20,12–19], composition of preparation mixture, preparation method, structure-directing agents, and preparation time and temperature predominantly control the zeolite morphology. Zeolites can be

prepared in a broad range of framework compositions based on zeolite formation chemistry [1]. In addition to the direct fabrication procedure, post-synthetic modification often offers an effective approach to improve the zeolites to display favorable characteristics. Powerful aspects of post-synthetic functionalization of zeolites, including reinsertion of heteroatoms into zeolite frameworks, ion-exchange, and synthesis of metal-supported zeolites, are discussed in the literature [21,22]. Newer treatment approaches will be addressed in the next sections.

Zeolite molecular sieves exhibit higher accessibility and remarkably higher selectivity and diffusivity resulting from their narrow pore aperture distribution [23]. Thus, this review initially addresses recent trends to improve the gas separation performance of zeolites themselves. The current approaches directed toward the enhancement of the carbon dioxide (CO_2) adsorption capacity of zeolites are considered. To realize the structure effect, the performance of zeolites with different structures, including nanoparticles and nanofibers on CO_2 adsorption, is also reviewed. Zeolite-based foams will be addressed to introduce ultra-high contents of zeolites for selective CO_2 capture. The remarkable improvement in polymeric membranes transport properties by incorporating pristine and functionalized zeolites is then considered. The inorganic sieve shape and size determine the interfacial adhesions between the polymer matrix and sieve. New structures of inorganic sieves have been prepared to design mixed matrix membranes (MMMs) with excellent gas separation performance. Of these, hollow zeolite spheres (HZSs) are reviewed. Employing nanoporous layered fillers, including AMH-3 and Jilin-Davy-Faraday, layered solid No. 1 (JDF-L1), has been summarized to overcome the limitation of adding high loadings of zeolites. In addition, this review touches on employing zeolitic imidazolate frameworks (ZIFs) in MMMs due to their exciting properties.

2. Zeolite-based adsorbents for CO_2 separation

Carbon dioxide (CO_2) gas which is mainly a byproduct of fossil fuel combustion, accounts for most of the greenhouse gas emissions to the atmosphere [25,26]. To reduce greenhouse emission, it is essential to separate CO_2 from a flue or exhaust gas that emanates from combustion plants. Therefore, CO_2 storage displays a potential approach for ensuring environmental sustainability and reducing CO_2 emissions. Post-combustion capture-based processes are employed mainly for separating CO_2 from flue gas. In this approach, four different techniques are explored immensely as frontier strategies to capture CO_2 after fossil fuel gets burnt: absorption, adsorption, membrane purification, and cryogenic distillation [27]. The widely utilized industrial technology for CO_2 capture is absorption-based, wherein amines are used. However, this process has many disadvantages, such as the high-energy requirement for amine solution regeneration and amines highly corrosive nature. On the other hand, adsorption has many compensations, i.e. low-energy requirements, low cost, and more applicable operating conditions. The choice of adsorbents represents a critical factor in effective CO_2 capture [28,29].

Zeolites are crystalline aluminosilicates that are implemented universally as highly efficient catalysts and sorbents [30]. Zeolites are commonly used as molecular sieves in CO_2 adsorption applications due to their tailorable cavities and pore sizes. The mechanism of the CO_2 adsorption process on zeolites has confirmed the physical adsorption of CO_2 molecules induced by firmly bound carbonate molecules by π-coordination or ion-dipole interactions [31]. Because of the strong interactions between the zeolitic cations and the stronger quadruple moment of N_2 compared with O_2, zeolites are applied in air separation applications. Compared with the other adsorbents, zeolite display characteristic performance, especially in the low-pressure regime, along with superior CO_2/N_2 selectivity [32,33]. Zeolites A, β, Y, 13X, ZSM, and chabazite are applied for separating CO_2 from N_2 [33]. Zeolites NaY and 13X are commonly employed in post-combustion CO_2 capture due to their high adsorption capacity, whereas zeolite NaA displays a high CO_2/N_2 selectivity due to its narrow pore size [33,34].

Interestingly, the pulsed current process was used by Akhtar et al. to synthesize thin and binder-less zeolite NaX laminates, with thicknesses, ranged between 310 and 750 μm and widths exceeding 50 mm [35]. The laminates offered a high CO_2 adsorption capacity as well as high CO_2/CH_4 and CO_2/N_2 selectivities. The adsorption characteristics of zeolites and their pore sizes can be tuned by varying the outer surface and modifying their crystal structure [30,36–41]. The several strategies utilized to chemically functionalize zeolites will be addressed in the following section below. Furthermore, auspicious improvement for the evolution of adsorption performance of zeolites by using nanoparticle and nanofiber particles will be discussed to investigate the structure effect. Moreover, the incorporation of ultra-high contents of zeolites for selective CO_2 capture, zeolite-based foams will also be reviewed.

2.1. Chemical modification of zeolites

Gas separation technologies that need a resolution in molecular size difference of 0.1 Å represent the main challenge in emerging renewable energy technologies. This concept includes CO_2 capture from flue gases and methane (CH_4) upgrading from biogas by separating hydrogen sulfide (H_2S) and CO_2. Both CO_2 capture and biogas upgrading can be accomplished effectively through temperature swing adsorption (TSA) or pressure swing adsorption (PSA) processes [25,42–44]. Lately, great attention has been given to design novel adsorbents with high adsorption capacity and selectivity for CO_2/N_2 and CO_2/CH_4 separations. At the heart of this concept, amine-grafted zeolites [45], mesoporous silica [26], amine-grafted silica [46], cation-exchanged zeolites [47,48], activated carbon [29], and MOFs [49,50] were employed. The next sections will describe the mainly used approaches to enhance the CO_2 adsorption on zeolites.

2.1.1. Amine-modified zeolites

Amongst different zeolites, zeolite 13X has been studied most because of its high CO_2 adsorption capacity. Zeolites are recognized to be less effective at high temperatures and more effective at ambient temperatures. To make zeolites more operative at high temperatures, amine-modified zeolites are proposed, in which both chemisorption and physisorption phenomena will take place [51]. Amine-impregnated adsorbents have attracted the researcher's interest because of the simple chemistry between the acidic CO_2 molecules and basic amine molecules incorporated onto the adsorbent external surface. The electron density and basicity of the nitrogen atom play a critical role in selecting an amine appropriate for CO_2 capture. Therefore, primary and secondary amines interact with CO_2 to produce ammonium carbamate [52].

Diffusion hindrance of impregnated amine molecules into the zeolite pores and pore blockage restricts achieving high CO_2 adsorption capacity [45,53,54]. This behavior is more critical for zeolites containing small pores (i.e. zeolite 4A) [55,56]. Hence, large pores containing zeolites such as NaY, 13X, and β are commonly applied in preparing amine-modified zeolites [45,53,57]. The binder-containing commercial zeolite 4A can be used for amine impregnation since it exhibits heterogeneous pore size distributions formed by the binder (such as attapulgite and kaolin), which offers an additional pathway for CO_2 diffusion into the zeolite pores [58]. It also provides enhanced CO_2 adsorption capacity and CO_2/N_2 selectivity [59].

Various amines have been applied in the preparation of amine-impregnated zeolites, including tetraethylenepentamine (TEPA), polyethyleneimine (PEI), and monoethanolamine (MEA) [60]. The CO_2 adsorption capacity in the temperature range of 30–120°C was measured for MEA-impregnated zeolite 13X, showing CO_2 capture efficiency was enhanced by a factor of 1.6 at 30°C and 3.5 at 120°C [51]. Recently, PEI of high molecular weight was impregnated on zeolite 13X by Karka et al. [60]. It was observed that the highest adsorption capacity was achieved at 75°C with 60 wt% PEI content (Fig. 2). Interestingly, Li et al. studied the effect of PEI molecular weight and type (branched or linear) on the CO_2 capture efficiency

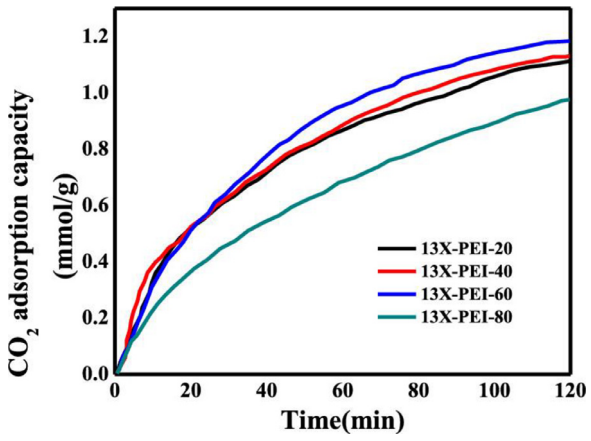

Fig. 2. CO_2 adsorption capacity as a function of time of various polyethyleneimine (PEI) contents on zeolite 13X at 1 atm and 75°C [60]. (For interpretation of the references to color in this figure legend, the reader is referred to the web version of this article.)

[61]. They reported that increasing PEI molecular weight reduced the CO_2 adsorption capacity, and linear PEI exhibited lower adsorption capacity than branched one because of chains restricted mobility. Other aliphatic amines such as butylamine, *iso*-butylamine, propylamine, and *iso*-propylamine also exhibit high affinity towards CO_2 molecules for the post-combustion CO_2 capture [52,62–64]. In this regard, the absorption capacity of *iso*-butylamine (0.78 mol of CO_2/mol of amine) is higher than that of MEA (0.72 mol of CO_2/mol of amine) for the post-combustion CO_2 capture [64]. The influence of the carbon chain length and steric hindrance of amines on CO_2 adsorption efficiency in amine-impregnated binder-containing zeolite 4A was discussed by Panda et al. [4]. They used pentylamine, *iso*-pentylamine, butylamine, *iso*-butylamine, propylamine, and *iso*-propylamine. Among these hybrid adsorbents, the *iso*-butylamine-modified adsorbent offered the highest adsorption capacity of 2.56 mmol/g at 1 bar and 25°C and significantly high CO_2/N_2 selectivity of 335. Moreover, Thakkar et al. synthesized different molecular sieves, including SAPO-34, Y, and ZSM-5 zeolites from kaolin clay [65]. The prepared sieves were treated with TEPA, and its impact on CO_2 uptake revealed that the TEPA-impregnated zeolite Y with 10 wt% TEPA displayed a higher CO_2 capacity than other zeolites owing to its larger mesopore volume. The mesopores present in the zeolite Y frameworks smoothed the accessibility of CO_2 molecules to the amine sites.

2.1.2. Silica-modified zeolites

In addition to gas separation applications, the silica modification process is applied for other uses as well, which includes catalysis [66], water treatment [67], and drug delivery [68,69]. The surface modification of zeolite alters the size of the pore entrance without influencing the internal morphology. In this context, an ultrathin alumina porous film was deposited on the surface of zeolite 5A particles by Yu et al. using the molecular layer deposition (MLD) process [39,70]. Moreover, the chemical vapor deposition (CVD) technique was applied to deposit a silica layer on mordenite to reduce the pore entrance sizes at 0.1 nm level [37]. Compared with CVD, the chemical liquid deposition (CLD) method is more scalable, amenable to finer tuning, and simpler to control [71,72]. The CLD approach is commonly applied to enhance catalyst performance. In this context, CLD modified zeolite ZSM-5 was used in the selective adsorption of disubstituted benzene isomers such as *m*-cresol/*p*-cresol and *m*-xylene/*p*-xylene [72]. In addition, Zhao et al. [40] reported the use of CLD modified zeolite ZSM-5 to remove dimethyl disulfide from methyl *tert*-butyl ether. Refrigerant mixtures consisting of R143a and R125 were separated using CLD modified zeolite 5A [41]. Recently, CLD modified zeolite 4A was used in the size-selective adsorption separation of CH_4 and CO_2 [73]. The zeolite 4A powder was modified with silicon tetrachloride as a silica precursor. These optimized zeolites offered a CO_2/N_2 selectivity of 44, a CO_2/CH_4 selectivity of 76, and an O_2/N_2 selectivity of 1.6 while maintaining high adsorption capacity.

The selective separation of CO_2 using commercial zeolites under humid conditions always suffers from many challenges. In the presence of water, zeolites always lose their adsorption property due to their higher affinity for water molecules, as in many real gas separation cases such as flue gases and biogases [74,75]. Thus, dehumidification is essential before CO_2 adsorption, which would dramatically increase the total energy consumption and the difficulty of the operation as well as the investment cost. In this context, the zeolites encapsulation with a shell can remarkably hinder the diffusion of water molecules into the zeolite core to preserve their CO_2 adsorption property in the presence of water [31]. In addition, a dynamic reaction-induced retardation behavior for moisture can be developed by considering amines for CO_2 separation. For instance, Liu et al. used sol-gel coating and PEI impregnation procedures to design core-shell zeolite 5A@mesoporous silica-supported-amine (5A@MSA) hybrid adsorbents for advanced CO_2 adsorption from flue gas in the presence of water [31]. The amino groups in the shell can react with CO_2 and H_2O molecules forming carbamate molecules, which will then be converted to bicarbonates or carbonates [26], efficiently retarding water diffusion and allowing CO_2 molecules to easily reach the zeolite core. The 5A@MSA hybrid adsorbent with 30 wt% of impregnated PEI displayed the highest CO_2 uptake. The PEI molecules are retained in the shell after 10 adsorption/desorption cycles, resulting in a very stable and efficient CO_2 adsorbent. Additionally, the same group coated zeolite 5A cores with a hydrophobic zeolitic imidazolate framework (ZIF)-8 shell to significantly minimize the moisture influence in CO_2 adsorption processes [76].

2.1.3. Ion-exchanged zeolites

Encompassing silicon and aluminum oxides, zeolites are recognized as microporous crystals exhibiting adsorptive and ion-exchange characteristics that tailor the interactions between adsorbents and adsorbates [77]. The impregnation of electropositive cations can improve the adsorption of acidic gases, and the introduction of alkali metal ions causes a remarkable improvement in the CO_2 adsorption performance [78]. Ammonium ion is often used due to its basic nature and affinity toward CO_2 molecules [45].

Diaz et al. modified parent NaX zeolites by using Na and Cs aqueous carbonate and hydroxide solutions as precursors [79]. Exchanging zeolite NaX with Cs has been demonstrated to increase the basicity of these zeolites. Cs-modified materials provided a higher CO_2 retention capacity than the Na-modified and parent zeolites. For Cs-treated zeolites, the desorption process took place at high temperatures in the range of 250–400°C, which results in interesting practical applications. In another investigation, Lee et al. [77] impregnated zeolite 13X with different alkali and alkaline earth metals, including K, Ca, and Mg, to investigate the surface interactions of the treated zeolites with CO_2 molecules. Additionally, the influence of moisture on the adsorption performance was also investigated. Particularly, the zeolite 13X modified with Ca showed the highest CO_2 adsorption efficiency, and the existence of moisture in the mixed gas flow decreased the capture performance. The adsorption equilibria of CH_4 and CO_2 in a cation-exchanged zeolite 13X was studied by Moura et al. [48]. Ion-exchange with Na^+, Li^+, NH_4^+, Ba^{2+}, and Fe^{3+} cations were performed in binderless zeolite 13X pellets. The adsorption capacity decreased in the following order: Na-NH_4 > Li > Ba for CH_4 and Li > Na > Ba-NH_4 > Fe for CO_2. The Li-exchanged zeolite showed higher CO_2 uptake than the Na-exchanged material because of lower adsorption enthalpy as well as higher selectivity and capacity.

Recently, Sun et al. investigated the use of transition metal ion-exchanged zeolite SSZ-13 for CO_2 adsorption [80]. Among the impregnated transition metal (Ag^+, Ni^{2+}, Co^{2+}, Zn^{2+}, Cu^{2+}, Fe^{3+}, La^{3+}, and Ce^{3+}) treated zeolites, the highest CO_2 capacities of 4.45 and 4.49 mmol/g and superior CO_2/N_2 selectivity of 42.61 and 52.55 were

Table 1
Discussed modified zeolite adsorbent materials.

Modification type	Zeolite type	Modifying reagent	CO_2 adsorption capacity	Ref
Amine	β	MEA, 40 wt%	At 1 atm and 303 K $\alpha = 1.76$, $\alpha' = 0.77$	Xu et al. [59]
	13X	MEA, 50 wt%	At 120°C $\alpha = 4$ mL/g, $\alpha' = 14$ mL/g	Jadhav et al. [51]
	13X	PEI, 60 wt%	At 1 atm and 75°C $\alpha = 0.36$, $\alpha' = 1.22$	Karka et al. [60]
	Binder-containing 4A	*iso*-butylamine, 0.3 wt%	At 1 bar and 25°C $\alpha = 2.20$, $\alpha' = 2.56$	Panda et al. [4]
	Y	TEPA, 10 wt%	At 25°C $\alpha = 0.9$, $\alpha' = 1.1$	Thakkar et al. [65]
Silica	4A	$SiCl_4$, 27 wt%	At 760 torr $\alpha = 4.3$, $\alpha' = 3.1$	Wang et al. [73]
	5A	TEOS/30 wt% PEI	At 298 K and 70% relative humidity $\alpha = 0.73$, $\alpha' = 5.05$	Liu et al. [31]
Ion-exchange	NaX	CsOH, 0.5 M	At 50°C, first cycle $\alpha = 2.22$ mg/g, $\alpha' = 12.97$ mg/g	Diaz et al. [79]
	13X	$Ca(CH_3COO)_2$, 1 M	Langmuir fitting, two-parameter model $\alpha = 1.21$, $\alpha' = 2.51$	Lee et al. [77]
	Binder-free 13X	LiCl, 1 M	At 1 bar and 298 K $\alpha = 6.27$, $\alpha' = 6.98$	Moura et al. [48]
	SSZ-13	$Co(NO_3)_2$, 0.5 M	At 1 atm and 273 K $\alpha' = 4.49$	Sun et al. [80]
	Clinoptilolite	$CaCl_2$, 0.2 M	Toth fitting $\alpha = 2.061$, $\alpha' = 1.911$	Kennedy et al. [47]

*α and α' are the adsorption capacities (mmol/g) of the pristine and modified zeolites, respectively.

achieved by using Ni^{2+} and Co^{2+} modified materials, respectively at 273 K and 1 atm. The outstanding adsorption efficiency can be attributed to the π-back-donation between transition metal cation sites and CO_2. Moreover, Kennedy et al. reported the adsorption performance of pure CO_2, N_2, and CH_4 gases on pristine, Cs^+, Ca^{2+}, and Fe^{3+} ion-exchanged clinoptilolite [47]. Ca-clinoptilolite exhibited the highest CO_2/CH_4 selectivity, whereas Cs^+ and Fe^{3+}-exchanged zeolites displayed a higher CH_4 adsorption equilibrium selectivity. The CH_4 capacity was deteriorated by blocking the pores in the Ca^{2+}-modified clinoptilolite. Table 1 summarizes the discussed modified zeolites in this review and the respective chemical reagents used in the modification process.

2.2. Zeolite nanoparticles

Designing of promising solid adsorbents with high CO_2 selectivity, high adsorption efficiency, and high thermal and mechanical stability are the foremost challenges in developing CO_2 separation by adsorption processes [81]. Decreasing the particle size reduces the diffusion pathways of adsorbate molecules and, consequently, improves the adsorption capacity [81,82]. Fabricating low-cost zeolite nanoparticles with a rapid capture and high adsorption capacity is in demand at a large-scale for CO_2 separations from flue gas [83].

Zeolite T is an intergrowth zeolite of offretite and erionite. Offretite and erionite exhibit varied structural configurations but are closely related to each other. The effective pore size of zeolite T is 0.36 nm, which is larger than the molecular size of CO_2 (0.33 nm) and smaller than the molecular size of CH_4 (0.38 nm) and N_2 (0.364 nm) [84,85]. However, the preparation of zeolite T nanoparticles is still limited. In this respect, Jiang et al. hydrothermally prepared highly recyclable zeolite T nanoparticles with a particle size of 150–200 nm for CO_2/CH_4 and CO_2/N_2 separations [81]. At 288 K and 100 kPa, the selectivity of CO_2/CH_4 and CO_2/N_2 reached 19.15 and 53.71, respectively. The nano-sized zeolite T particles adsorption capacity was 30% higher than that of the micron-sized ones at 288 K and 100 kPa.

Many concepts have been designed to prepare zeolite nanocrystals with and without using morphology-directing materials [86–90]. Of these, zeolite NaA nanocrystals with high CO_2 adsorption capacity were synthesized by template-free hydrothermal preparation in thermo-reversible methylcellulose gels [83]. The thermo-gelation of methylcellulose in the alkaline Na_2O-SiO_2-Al_2O_3-H_2O system performed a vital role in determining the particle size. Compared to the commercial micro-level zeolite NaA, the synthesized nanocrystals with a particle size of 100 nm offered a relatively rapid CO_2 capture and high adsorption capacity of 4.9 mmol/g at 100 kPa and 293 K.

As mentioned previously, the ion-exchange can be used to tailor the zeolite pore size [36]. In this context, the kinetic CO_2/N_2 selectivity can be induced by diminishing the window aperture of zeolite NaA by K^+ cation-exchange as N_2 has a larger kinetic diameter than CO_2 [34]. For the 17.3 atomic% zeolite NaKA, the selectivity was increased by a factor of 5–10 when compared with zeolite NaA. Because of the narrow pore size, CO_2 diffusion will be retarded among the cages in zeolite NaKA. Depending on crystal quality and decreasing the particle size, the diffusion rate can be quadratically increased [91]. Furthermore, zeolite NaKA nanoparticles were prepared by Cheung et al. and the CO_2 adsorption rate on nano-sized zeolites NaA and NaKA did not increase significantly [91].

2.3. Zeolite-based nanofibers

The electrospinning technique is considered one of the most prominent strategies to synthesize thin, continuous, and novel nanofibers for numerous applications [92–94]. Nanofibers with desired characteristics such as high surface area, porosity, and diameters ranging from tens of nanometers to few micrometers can be designed using electrospinning. For instance, enhancing the gas separation performance of acrylonitrile butadiene styrene fibers by incorporating 10 wt% of natural zeolite, which was reported by Calderon et al. [95]. The catalytic cracking of isobutane was stimulated by adding 34 wt% of zeolite ZSM-5 to poly(vinylpyrrolidone) (PVP) nanofibers [96].

Furthermore, the zeolite/polymer nanofibers fabrication step can be performed initially, and then afterward, the thermal surface etching process ranging from 250 to 450°C can be applied for eliminating the polymer matrix and designing zeolite nanofibers exhibiting high surface area [97]. The thermal etched zeolite Y nanofibers at 400°C offered a specific

Table 2
The BET surface area and pore size of the zeolite Y powder and zeolite Y nanofibers with varied thermal etching temperatures [97].

Sample	BET surface area (m^2/g)	Pore size (nm)	t-plot micropore volume (cm^3/g)
No thermal etching	210	20.5	0.04
300°C thermal etching	586	14.5	0.20
350°C thermal etching	676	14.0	0.21
400°C thermal etching	816	13.7	0.25
Zeolite Y powder	861	23.7	0.24

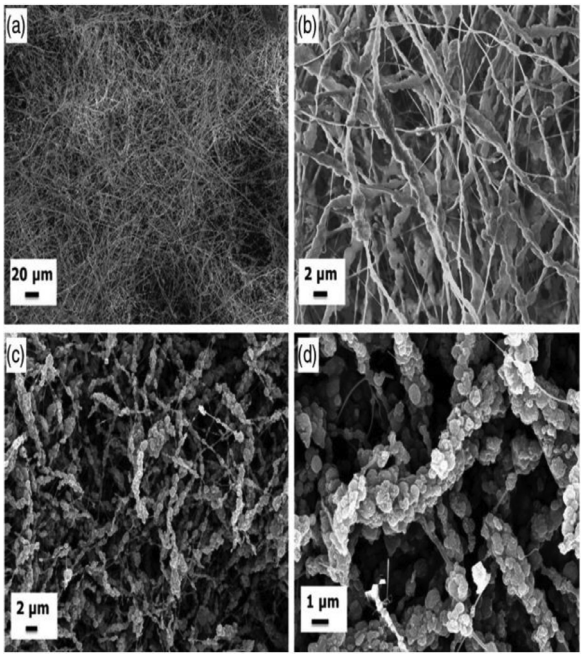

Fig. 3. SEM micrographs of (a,b) ZSM-5/ poly(vinylpyrrolidone) (PVP) nanofibers; (c,d) ZSM-5/C nanofibers [98].

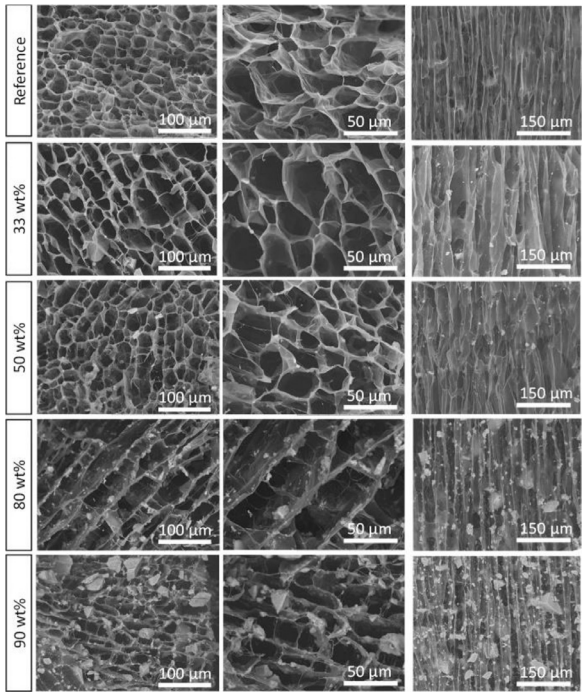

Fig. 4. SEM micrographs of the foams with different contents of silicalite-1. The anisotropic structure was confirmed from the cross-sectional micrographs (right column) [99].

surface area of 816 m^2/g, close to that of zeolite Y powder (Table 2) [97]. It is worth mentioning that the zeolite Y nanofibers surface area and pore size can be tuned by changing the thermal etching temperature (see Table 2) [97].

Few researchers discussed the structuring of zeolite nanofibers with a polymeric carrier and modifying the morphology by post-processing for gas separation applications. For biogas upgrading, Zhang et al. reported the synthesis of hierarchical zeolite nanofibers from a commercial zeolite ZSM-5 nanopowder and PVP [98]. ZSM-5/carbon (ZSM-5/C) composite nanofibers were then obtained by carbonizing the electrospun ZSM-5/PVP nanofibers at 700°C under N_2 gas flow. The ZSM-5/C nanofibers displayed a 30.4% increase in the surface area relative to the pristine ZSM-5 nanopowder. A CO_2 adsorption capacity of 2.15 mmol/g and CO_2/CH_4 selectivity of 20 were achieved at 1 bar and 293 K. Fig. 3 demonstrates the SEM micrographs of the spun ZSM-5/PVP composites before and after carbonization. Afterward, the carbonized nanofibers were processed into hierarchical porous pellets (with a porosity of ~ 60%) to produce efficient adsorbents with a CO_2 adsorption capacity of 3.18 mmol/g at 4 bar and 293 K after 5 adsorption-desorption cycles.

2.4. Zeolite-based foams

It is well-documented that microporous crystalline aluminosilicates (with a pore size less than 2 nm) in the form of zeolites represent a potential candidate for CO_2 adsorption in the eminent battle against climate change and global warming phenomena. The poor processability of conventional zeolite powders limits their engagement in many gas filtration industrial applications [99]. To address this restriction, Valencia et al. recently developed hybrid foams using meso/macroporous gelatin/nanocellulose supporting materials, which can sustain ultrahigh contents of silicalite-1 up to 90 wt%, without the necessity of adding any crosslinker [99]. The hierarchical meso/macro-porosity improved gas molecules diffusion and limited the pressure drop over the adsorbent permitting the high gas flow rates. Thus, the strong gelatin/nanocellulose networks effectively preserved the zeolite crystals efficiency without blocking their pores. Fig. 4 demonstrates the preserved anisotropy of the foams even at high contents of zeolite. Examining the hybrid foams revealed the linear relationship between CO_2 uptake and zeolite loading with high CO_2/N_2 selectivity. The reusability of these foams displayed a minor reduction in adsorption efficiency. This novel design offered the best overall combination of adsorption and mechanical characteristics for the 90 wt% loaded zeolite foams. In another work, Mazaj et al. [100] embedded zeolite nanocrystals in the walls of microcellular carbon foams providing unique textural features, which resulted in improved CO_2 uptake due to the existence of ultramicropores. This synergism delivered a novel adsorbent with a CO_2/N_2 selectivity of 80 and an outstanding multi-cycle adsorption performance under humid environments (70% efficiency preservation after 30 regeneration cycles). More interestingly, the framework allowed Joule heating and cooling, and consequently, an energy-efficient regeneration process with a projected energy consumption of only 12 kWh was possible.

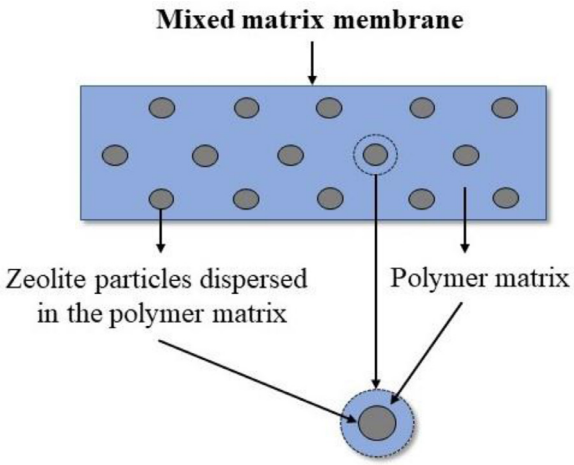

Fig. 5. Schematic illustration of a typical mixed matrix membrane (MMM). (For interpretation of the references to color in this figure legend, the reader is referred to the web version of this article.)

3. Zeolite/polymer mixed matrix membranes (MMMs) for gas separation

Natural gas mainly consists of CH_4, with small amounts of other hydrocarbons comprising ethane (C_2H_6), propane (C_3H_8), and butane (C_4H_{10}), as well as some impurities including CO_2, H_2S, N_2, and O_2 [101]. To avoid pipeline corrosion and meet pipeline quality standard specifications, CO_2 gas must be separated [102]. As mentioned before, technologies used for CO_2 separation applications include membranes, adsorption, absorption, and cryogenic distillation [27]. In addition to adsorption, membrane separation technologies attracted great interest over the years due to low energy demand, low capital cost, and simple operation, with polymeric materials revolutionizing membrane technology [103–105], followed by inorganic membranes [106,107] and mixed matrix membranes (MMMs) [108,109]. MMMs have gained the most attention as polymeric membranes face a trade-off between gas selectivity and permeability (known as the Robeson upper-bound limit) [110], while inorganic membranes are hindered by poor reproducibility and high production cost [111]. MMMs consist of two or more different materials (polymer matrix and filler particles), each with different fluxes and selectivity [112]. The filler particles get dispersed into the continuous phase of a polymeric network. Fig. 5 demonstrates a general illustration of a typical MMM. The polymer matrix should develop strong linkages with the filler galleries in the membrane and facilitate high gas selectivity with good mechanical and thermal characteristics [113]. Frequently applied polymers in gas separation applications involve Pebax [114–116], Matrimid [117–120], polysulfone (PSF) [121–123], and 6FDA-based polyimides [124–126]. Meanwhile, many fillers concerning zeolites [127–129], MOFs [115,125,126,130–132], and carbon materials [122,133,134], are extensively addressed in the literature. Moreover, gas selectivity of membranes has been observed to improve remarkably by incorporating small amounts of molecular sieves. This behavior was due to the higher separation efficiency of the molecular sieve than the neat polymer, and thus the MMMs efficiency surpassed the Robeson upper-bound limit. In other developments, MMMs have been designed to enhance polymers mechanical and electrical characteristics [135–137].

3.1. Gas transport in polymeric membranes

The gas transport property arises when gas molecules diffuse across the networks via cavities in the polymer and dissolve into the membrane surface. Notably, the permeability arises from the contribution of these two processes, as described in Eq. (1).

$$P = D.S \tag{1}$$

Where; P is permeability (which relates to the gas partial pressure), D is the diffusion coefficient (kinetic factor), and S is the sorption coefficient (thermodynamic factor). The sorption coefficient relates to the physicochemical characteristics of the materials and the gas condensability. Henry's law describes the direct proportionality between the amount of gas dissolved in a polymer and the partial pressure, while Fick's law expresses the diffusion coefficient [138]. The diffusion coefficient describes the energy required for the gas molecules to pass through the polymer. This factor is also controlled by the shape and the size of the guest gas molecules [139]. The ideal selectivity (α) is also used to evaluate the networks gas transport properties (Eq. (2)). Certainly, the selectivity is described as the ratio of the permeability for gases x and y. From Eq. (1), the selectivity can be expressed using diffusion selectivity (ratio of diffusivity coefficients) and adsorption selectivity (ratio of sorption coefficients), as shown in Eq. (2) [138].

$$= \frac{P_x}{P_y} = \frac{D_x}{D_y}.\frac{S_x}{S_y} \tag{2}$$

Therefore, as studied, the pure polymeric membranes description will vary when introducing zeolites into the polymer networks. Additionally, the interfacial adhesions between zeolite surfaces and polymer networks that represent a vital role in controlling the membranes gas separation performance will be discussed well in the next section.

3.2. Interphase morphologies of MMMs

The synthesis of defect-free MMMs demonstrates a significant challenge in improving its separation performance. Great devotion has been given to design MMMs with novel properties such as inorganic filler excellent dispersion, developed interfacial adhesions between the polymer matrix and inorganic filler, appropriate particle dimensions, and suitable content of inorganic filler. Inadequate sieve dispersion in the polymer matrix attributes to agglomerate formation and worsening of the separation performance in MMMs, primarily while using high proportions of the inorganic sieve [140]. Weak adhesion interactions develop interfacial voids, rigidified polymers, and pore blockage [141]. Moreover, inappropriate particle dimensions and excess content of inorganic fillers create pinholes and voids, resulting in the deterioration of membranes [108,142]. Thus, intensive interest should be devoted to unraveling these challenges using the introduction of modification strategies.

Two parameters are highly significant to the interphase formation: (i) the stress that arises during the fabrication of MMM and (ii) the nature of polymer-zeolite interactions [117]. The nanoscale interface morphology of inorganic/organic MMMs plays a critical role in controlling the gas separation performance of MMMs. There are four different structures (Fig. 6) [108]: (a) Case 1 is an ideal case (defect-free) but difficult-to-obtain morphology, corresponding to Maxwell model prediction. (b) Case 2 displays interfacial voids as a result of the detachment of polymer galleries from the zeolite surface. (c) Case 3 shows the rigidified polymer chains in direct contact with the zeolite surface. (d) Case 4 indicates the partially sealed zeolite pores by the rigidified polymer galleries.

Interfacial voids between the filler and polymer phases act as a bypass for the gas molecules around the sieve particles and can affect the gas selectivity of the fabricated membranes [103,143–148]. This problem is critical, especially for zeolites, as they exhibit poor compatibility with the organic polymers [23]. The rigidified polymer layers around the sieve may create a region with less free volume and restricted chain mobility, resulting in a decrease in permeability [149,150]. The partially sealed zeolite pores by the rigidified polymer chains may also lead to a permeability reduction [145,151,152]. Although polymer rigidification [153–156] and partial pore blockage [150] can improve the gas selectivity by enhancing the diffusion selectivity, it is hugely abstruse to control, characterize, and evaluate them.

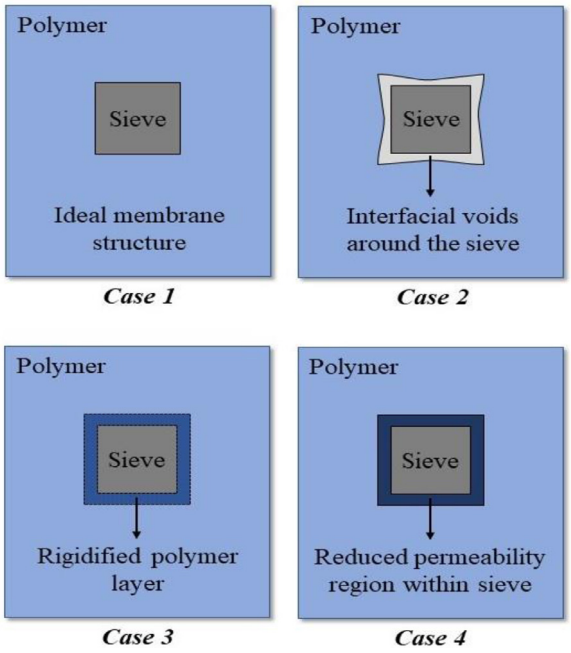

Fig. 6. Illustrative scheme of possible structures of mixed matrix membranes (MMMs). (For interpretation of the references to color in this figure legend, the reader is referred to the web version of this article.)

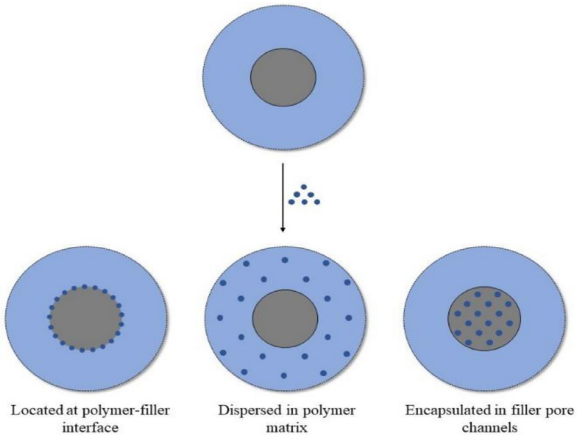

Fig. 7. Illustrative scheme of possible structures of the third component in ternary mixed matrix membrane (MMM) systems. (For interpretation of the references to color in this figure legend, the reader is referred to the web version of this article.)

3.2.1. *Improving interfacial adhesion*

Several approaches have been employed to adjust the interfacial morphology between the polymer and the sieve and control the dispersion of the sieve particles in the polymer network [23,144,157–161]. The widely used concepts include heat treatment, priming, and ternary MMM systems preparation via chemical and physical treatments of fillers [162–164].

Thermal annealing is the most economical and the most simple post-treatment process to remove the remaining solvents and discharge the stress from MMMs [165]. This process describes the membranes annealing at temperatures close to their glass transition temperature (T_g) under vacuum [103]. Thermal annealing improves polymer chains mobility, increases the free volume, and subsequently develops the adhesion between the polymer and filler [103]. For clarifying, Bakhtiari et al. [166] thermally annealed membranes to develop the adhesions between zeolites (4A and ZSM-5) and polymers (Matrimid®5218 and P84). The cooling procedure after the heat treatment process is critical to prevent voids formation. In this regard, natural and immediate quenching cooling processes can be used [23]. Natural cooling processes cause excellent interfacial adhesions as the polymer chains are frozen and hardened gradually with decreasing temperature. Meanwhile, the immediate quenching cooling method results in detaching the polymer chains from the filler surface due to the fast freezing of polymer chains. A case in point, Li et al. synthesized zeolite (3A, 4A, and 5A)/polyether sulfone (PES) MMMs with excellent adhesions after annealing the membranes at 250°C for 12 h [150]. The interfacial adhesions in MMMs that processed under natural cooling conditions were better than those in MMMs that processed with immediate quenching.

In addition to the thermal annealing method, the priming process includes adding a small quantity of polymer solution (usually 5–10 wt%) to the inorganic sieve before incorporating it into the bulk polymer [167]. The surface of the filler will be encapsulated with a thin layer of polymer. This process aims to reduce the stress created at the polymer-filler interface, improve the compatibility, weaken the agglomeration propensity of filler particles (especially at high contents), and minimize interfacial defects [23,168]. For instance, the compatibility of carbon molecular sieve with Ultem®1000 and Matrimid®5218 was enhanced by Vu et al. [169] using this technique at high contents up to 35 wt%. Moreover, zeolite SSZ-13 was primed with propanediol monoester cross-linkable (PDMC) polymer for improved interfacial adhesions [168].

Incorporating a third material into binary MMM systems appears to be an additional strategy. The third material can either be located at the filler-polymer interface, be distributed in the polymer matrix, or encapsulated in the filler pore channels (Fig. 7) [170]. For instance, the third component positioned at the polymer-filler interface can bind the borders or fill-in the voids, as demonstrated in Fig. 8 [170]. The silanization method is commonly applied to chemically improve the filler surface using silane coupling agents [127,149,162,171]. These agents are capable of linking the inorganic filler to the polymer network [172]. According to Fig. 9, the silane groups first react with the hydroxyl groups attached to the inorganic filler surface. Afterward, the Y group in the silane group bonds with the polymer chain resulting in developing the adhesion interactions between the polymer matrix and the filler [173,174]. To preserve the inorganic sieve pores unblocked after the silanization procedure is crucial to guarantee the filler particle ability to display their gas transport properties. For clarifying, 3-aminopropyldiethoxymethylsilane (APDEMS) was used for improving the surface of zeolite A for developed adhesions with PES chains [149]. The addition of different third materials and the corresponding influences on the performance of CO_2 separation is visualized in Table 4 and will be addressed comprehensively in Section 3.4 (modified zeolite/polymer MMMs).

3.3. *Pristine zeolite/polymer MMMs*

Recent trends in membrane separation technology have heightened the requirements for the membranes to have a promising separation performance [175–178]. The membrane separation technology is utilized mainly to design unique membranes exhibiting high selectivity and permeability. In this respect, the selectivity and permeability can be increased by incorporating the right zeolite in the polymer matrix. Zeolites are used commonly in gas separations because of their pore angstrom size and crystalline morphology.

Poly(dimethylsiloxane) (PDMS) with a repeating unit of [-O-$Si(CH_3)_2$-] is well employed in membrane fabrications for gas transport applications [179–182]. Additionally, the PDMS mechanical characteristics are enhanced significantly by incorporating inorganic fillers such as zeolites [183]. Different molecular sieves such as NaA, NaX, silicalite-1, and graphite were used by Clarizia et al. [151] for increasing the selectivity and diminishing the permeability of the PDMS matrix for certain gas pairs. Tantekin-Ersolmaz et al. discussed the impact of

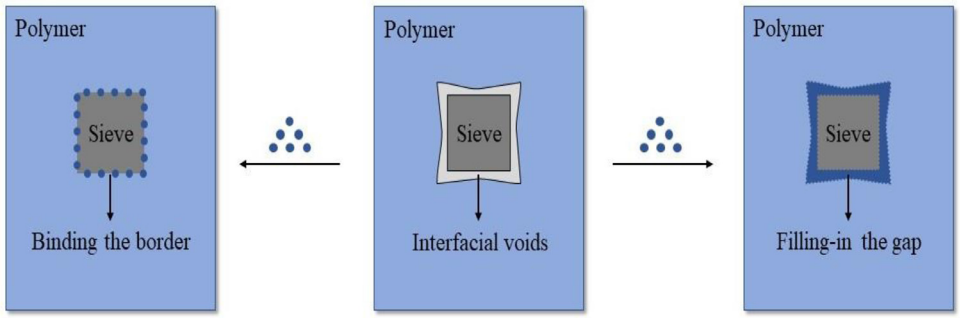

Fig. 8. Illustrative scheme of interfacial voids healing by the third component. (For interpretation of the references to color in this figure legend, the reader is referred to the web version of this article.)

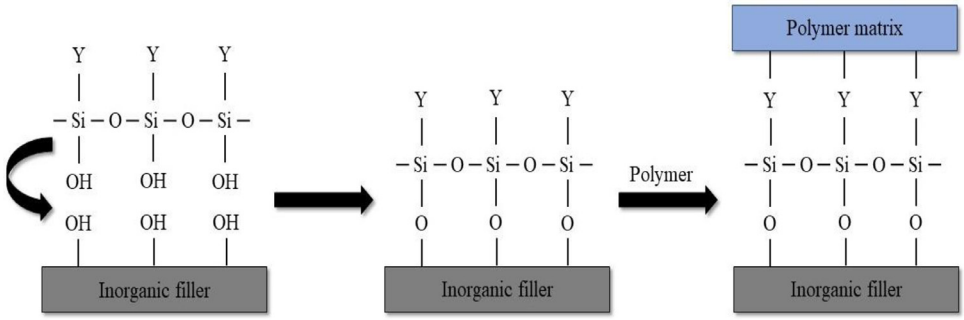

Fig. 9. Reaction mechanism of silane coupling agent. (For interpretation of the references to color in this figure legend, the reader is referred to the web version of this article.)

zeolite particle size on gas permeability of zeolite-PDMS MMMs [184]. Increasing the zeolite particle size was observed to increase the permeability while selectivity was less affected. Moreover, zeolite ZSM-5, in addition to the PDMS matrix, enhanced remarkably the permeability of both single and mixture gases [185]. Silicon and fluoro silicon/zeolite 4A membranes improved the water selectivity and permeability [183]. The influence of zeolite 4A nanoparticles incorporation in PDMS matrix was evaluated by Rezakazemi et al. [186]. The MMMs offered both higher H_2/CH_4 selectivity and H_2 permeability comparatively to the neat PDMS membrane.

Zeolite and carbon molecular sieves can be utilized to improve the selectivity of rubbery polymers that are poorly effective for CO_2/CH_4 mixtures [187]. Poly(vinyl acetate) (PVAc) was used as the host matrix to synthesize highly loaded zeolite 4A MMMs [188]. For 50 vol% zeolite containing membrane, the CO_2 selectivity was increased by 63% while permeability remained unaffected. Tahir et al. [189] tuned the gas transport properties of fluorinated-sulfonated poly(ether ether ketone) (F-SPEEK) membranes by impregnating zeolite 4A. The membranes were synthesized with a degree of 40% sulfonation. Besides, due to the polymer's intrinsic nature and modified membrane structure because of filler addition, the introduction of zeolite 4A improved both selectivity and permeability. The maximum selectivity for CO_2/N_2 and CO_2/CH_4 were 58 and 55 compared to 51 and 47 for the pure polymer, respectively, and the maximum CO_2 permeability was 49.2 Barrer with incorporating 30 wt% of zeolite 4A. With adding zeolite 4A, the membrane intrinsic CO_2 solubility was declined from 10.7 to 1.9 (10^{-2}) cm^3 (STP)/cm^3 cmHg. Recently, Afarani et al. [190] addressed the influence of zeolite ZSM-5, 3A, and 4A on the gas transport properties of zeolite-polyurethane (PU) MMMs. The permeability of all gases and the selectivity of CO_2/CH_4, CO_2/N_2, and O_2/N_2 gas pairs were increased with increasing the zeolite loading. The PU membrane containing 12 wt% of zeolite 4A displayed the highest permeability and CO_2/CH_4, CO_2/N_2, and O_2/N_2 selectivity. Furthermore, Mohamad et al. incorporated zeolite T particles into PSF membranes to improve the separation of CO_2 from CH_4 [121]. The CO_2 permeability was increased from 12.33 GPU for the neat PSF membrane to 82.30 GPU after adding 4 wt% of zeolite T particles; meanwhile, the highest CO_2/CH_4 selectivity reached 3.37 after incorporating 3 wt% of zeolite T particles. Murali et al. [114] introduced zeolite 4A into a

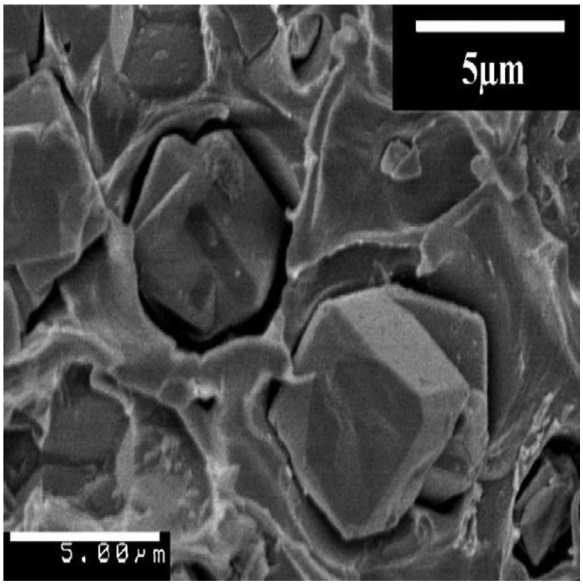

Fig. 10. SEM micrograph of zeolite particles showing a "sieve-in-a-cage" structure [168].

Pebax-1657 matrix. It was revealed that increasing zeolite 4A content enhanced the permeability but suppressed selectivity due to the creation of microscopic interfacial voids between Pebax and zeolite 4A phases. Non-selective interfacial voids can be formed due to the poor adhesion forces at the polymer-zeolite interfaces. These voids, which increase the permeability of the MMMs and diminish the selectivity, are identified as a "sieve-in-a-cage" structure [191,192]. Hillock et al. observed such voids by introducing zeolite SSZ-13 into a cross-linked polyimide (PI) modified with 1,3-propanediol (Fig. 10) [168]. These voids locate the membrane performance above the Robeson upper-bound limit, and the membrane selectivity of CO_2/CH_4 increased up to 47 with enhanced CO_2 permeability (89 Barrer). Fernández-Barquín et al. [193] achieved good compatibility between poly(1-trimethylsilyl-1-propyne) (PTMSP)

and zeolite A to synthesize void-free membranes. Zeolite A was first well blended with PTMSP and then coated on a support material in both hollow fiber and flat forms. The hollow fiber support was made from PSF, while the flat sheet support was fabricated from PES. They realized that the permeability of CO_2 gas increased with sustained selectivity in both membrane designs. The chemical modification of zeolites is observed to enhance their compatibility with the polymer matrices, as discussed in the next section.

3.4. Modified zeolite/polymer MMMs

Fabricating MMMs offers many challenges, including polymer rigidification, agglomeration, and non-uniform distribution of inorganic fillers as well as incompatibility between polymer and filler [194]. These challenges have led to a new strategy by functionalizing fillers for better gas separation efficiency than the membranes loaded with non-functionalized fillers [115,195–198]. The chemical functionalization reduces agglomerates formation, which creates the non-selective interfacial voids between the polymer and sieve and improves the membrane homogeneity [113].

As mentioned before, zeolite surface modification plays a vital role in adjusting the pore size without changing internal morphology. For example, Yong et al. employed 2,4,6-triaminopyrimidine (TAP) to strengthen the adhesion interactions between zeolite galleries and PI matrices via hydrogen bonding [163]. The TAP amount needed for reducing the formation of the voids was observed to be in the order of zeolite NaSZ390HUA > 5A > NaY > 4A ≈ 13X. Therefore, void-free TAP/PI/zeolite 4A membranes revealed lower N_2, O_2, CH_4, and CO_2 permeabilities than the PI/zeolite 4A MMMs. In contrast, TAP/PI/zeolite 13X MMMs offered the opposite behavior with negligible permselectivity (which denotes the permeability of a mixture of gases). Furthermore, APDEMS was applied to improve the zeolite surface for developed adhesions between zeolites (3A, 4A, and 5A) and PES chains [149]. Increasing modified zeolite 4A content diminished the membrane permeability of all gases, whereas the permeability of modified zeolite 5A MMMs initially declined and then increased at greater zeolite concentrations (Fig. 11). This behavior can be attributed to the presence of CH_2 and CH_3 groups [149].

Ion-exchange treatments of zeolites can be applied to develop the chemical and physical adsorption properties of penetrants in the zeolites [199]. By introducing Ag^+ ions, Li et al. increased the CO_2 permeability of PES/zeolite NaA membranes [199]. Increasing zeolite AgA loadings reduced the CO_2 permeability due to PES chains rigidification and blocking zeolite pores. Because of molecular sieving effects, the CO_2/CH_4 selectivity increased with increasing zeolite content and reached a maximum of 59.6 at 50 wt% of contents. Amooghin et al. performed ion-exchange to incorporate Ag^+ ions into zeolite NaY to improve the adhesion between Matrimid®5218 and zeolite for CO_2/CH_4 separation [200]. The CO_2/CH_4 selectivity of the AgY(15 wt%)/Matrimid MMM increased by ~ 66% relative to pure Matrimid (60.1 vs 36.3, respectively). Additionally, CO_2 permeability improved by ~ 123%, from 8.34 Barrer for the pure membrane to 18.62 Barrer. These gas transport properties are privileged and so they can be attributed to combining the intrinsic surface diffusion effect of zeolite Y with the facilitated transport of Ag^+ ions. Moving forward, the same research group developed novel hybrid host-guest nanocomposites by coating a metal-organic complex of transient metal (polyaza macrocyclic Co-ligand complex) in zeolite Y cavities ($[Co(tetra\text{-}aza)]^{2+}$-NaY) using the process of "ship-in-a-bottle" [201]. Afterward, the encapsulated zeolite was incorporated into the Matrimid®5218 network to design unique MMMs for gas transport applications. The novel membrane with 15 wt% of encapsulated zeolite Y at 2 bar and 35°C demonstrated a CO_2/CH_4 selectivity of 111.6 and CO_2 permeability of 18.96 Barrer, which were more than three- and two-fold that of neat polymer efficiency. Returning to the ion-exchange strategy, Luna et al. [202] conducted ion-exchange of Na^+-clinoptilolite with Ca^{2+} ions using an aqueous solution of $CaCl_2$ to develop the gas transport properties of polyether block amide Pebax®2533 (PEBA) for $CO_2/N_2/CH_4$ ternary gas mixture separation. The Ca^{2+}-exchange modification was achieved on the zeolite surfaces and in cavities without any microstructural change. The incorporation of clinoptilolite enhanced the permselectivity properties of the MMMs for gas separation compared with the neat polymeric membrane. The strong quadrupolar momentum interactions with the electrostatic field that were formed by Ca^{2+} ions resulted in a selectivity six times greater than that of the neat polymer.

Recently, MMMs comprising clinoptilolite zeolite and PSF were synthesized by Castruita-de León et al. [203]. The zeolite was impregnated with three alkyl amines, including PEI, bis(2-hydroxypropyl)amine (BHPA), and ethanolamine (EA). The MMMs containing EA-modified zeolite offered an enhancement of up to 55% on the CO_2/CH_4 selectivity and 30% on the CO_2 permeability compared with the neat PSF membrane. They also revealed that the membranes containing BHPA-modified clinoptilolite showed the highest selectivity. To evade the competitive adsorption of moisture, Junaidi et al. [204] introduced fluorocarbon-modified zeolite SAPO-34 into the PSF matrix using 1H,1H,2H,2H-perflourodecyltriethoxysilane (HFDS) to convert the hydrophilic zeolite SAPO-34 into a hydrophobic one. It was revealed that the fluorocarbon functionalization caused a minimum effect on the CO_2 uptake and surface area of zeolite SAPO-34. After functionalization, the membrane hydrophobicity increased by ~ 17.64%, while water contact angle on zeolite SAPO-34 increased from 33° to 130°. The membrane containing 10 wt% of zeolite modified with 1 weight ratio of HFDS (PSF-10/HFDS 1.0) displayed enhanced adhesion interactions between the PSF matrix and zeolite galleries, reducing the formation of the interfacial voids. The CO_2 permeance of this membrane was increased to 278.8 GPU with ideal CO_2/CH_4 selectivity of 38.9 compared to the membranes with unmodified filler and neat PSF membrane. Moreover, the PSF-10/HFDS 1.0 membrane gas selectivity under wet conditions was very close to its dry mixed-gas selectivity. The mixed-gas separation efficiency for PSF-10/HFDS 1.0 membrane remained sustained during the long-hour run in both wet and dry environments. On the other hand, the membrane with 10 wt% of unmodified zeolite SAPO-34 showed a more than 90% decrease in the separation efficiency under wet mixed-gas conditions. Furthermore, Ahmad et al. used an acetate-based ionic liquid (1-butyl-3-methylimidazolium acetate) to develop the adhesions between zeolite SAPO-34 and PSF matrix in the MMM synthesized through phase inversion [205]. The interfacial sealing by ionic liquid improved the CO_2/N_2 selectivity up to ~ 818% relative to the unmodified MMM. The highest CO_2/N_2 selectivity of 39.6 was reached by impregnating 5 wt% of zeolite SAPO-34 treated with 0.4 M of the ionic liquid. In another design, Maleh et al. designed a functional moderate selective layer MMM which included a moderate Pebax layer mixed with COOH-modified zeolite NaX nanoparticles over a microstructure PES support layer [206]. The addition of COOH-modified zeolite to the polymer network displayed enhanced dispersions and interactions over unmodified zeolites. Incorporation of COOH-zeolite up to 15 wt% increased the CO_2 permeability to 187.76 Barrer, and CO_2/CH_4, CO_2/N_2, and CH_4/N_2 selectivities to 57.41, 288.86, and 5.03, respectively (measured at 6 bar). As shown below, Tables 3 and 4 compile the gas transport properties of pristine and modified zeolite MMMs.

3.5. Zeolite-like/polymer MMMs

3.5.1. Hollow zeolite spheres (HZSs)/polymer MMMs

The filler shape and size represent important factors in determining the interfacial adhesion between the filler and polymer network [207–209]. New structures of inorganic fillers have been designed to fabricate looked-for MMMs with improved gas transport properties. Of these, hollow zeolite spheres (HZSs) were designed for minimized agglomeration and enhanced distribution of filler particles in the polymer network, especially when using microparticles [210–212]. This behavior can be attributed to the spherical shape of the filler particles, which enhances the polymer/filler contact, and microparticles can be used to minimize

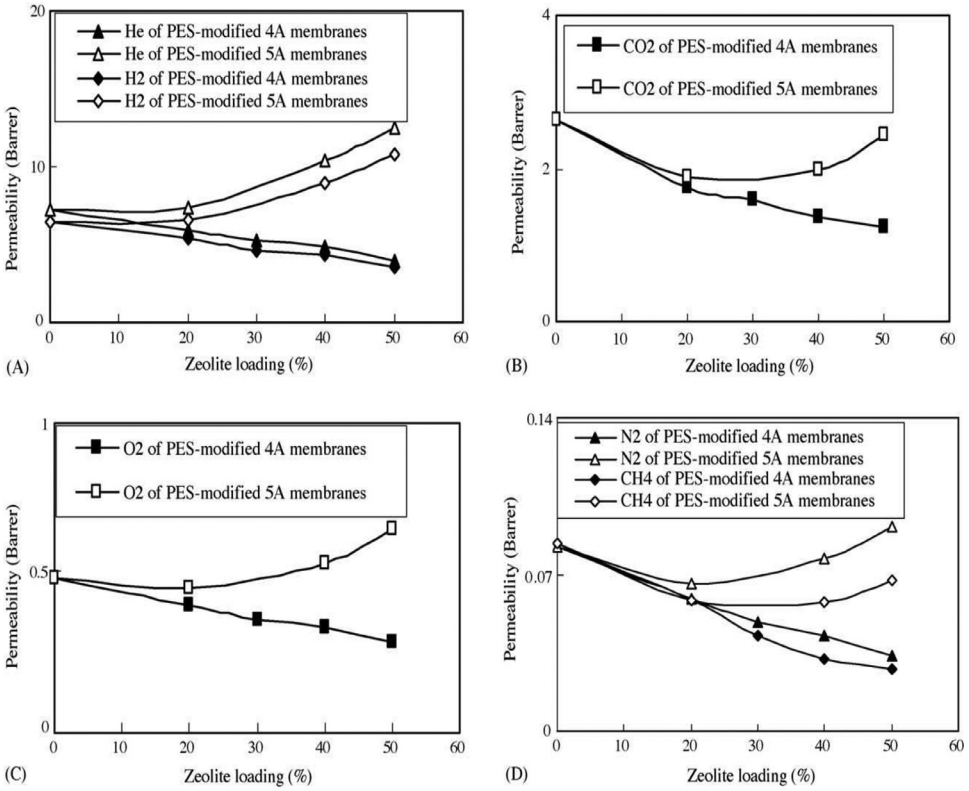

Fig. 11. Zeolite content influence on gas permeability of polyethersulfone (PES)-based mixed matrix membranes (MMMs) containing amino-modified zeolites 4A and 5A [149].

Table 3
Summary of gas transport properties of pristine zeolite-based MMMs.

Gas type	Host matrix	Zeolite type	Membrane performance Neat polymeric membrane	Mixed Matrix Membrane	Ref
CO2/CH4 at 60 oC	PDMS	Silicalite-1, 50 wt%	αCO2/CH4 = 2.60	αCO2/CH4 = 3.90 P = 3610	Clarizia et al. [151]
CO_2/N_2	PDMS	ZSM-5, 66 wt%	$\alpha_{CO2/N2}$ = 11.1 P = 3499	$\alpha_{CO2/N2}$ = 11.1 P = 11,648	Hussain et al. [185]
CO_2/CH_4	PDMS	4A, 40 wt%	$\alpha_{CO2/CH4}$ = 3.11 P = 4968	$\alpha_{CO2/CH4}$ = 3.09 P = 3208	Rezakazemi et al. [186]
CO_2/CH_4 (10% mol CO_2, 40 psia)	PVAc	4A, 50 vol%	$\alpha_{CO2/CH4}$ = 33.5 P = 2.15	$\alpha_{CO2/CH4}$ = 49.4 P = 4.33	Adams et al. [188]
CO_2/CH_4	PU	4A, 12 wt%	$\alpha_{CO2/CH4}$ = 5.89 P = 69.01	$\alpha_{CO2/CH4}$ = 7.38 P = 81.63	Afarani et al. [190]
CO_2/CH_4	PSF	T, 4 wt%	$\alpha_{CO2/CH4}$ = 2.63 P = 12.33 GPU	$\alpha_{CO2/CH4}$ = 2.64 P = 82.30 GPU	Mohamad et al. [121]
$CO_2/CH_4/N_2/O_2$	Pebax-1657	4A, 30 wt%	$\alpha_{CO2/CH4}$ = 18 $\alpha_{CO2/N2}$ = 40.2 $\alpha_{O2/N2}$ = 3.4 P = 55.8	$\alpha_{CO2/CH4}$ = 7.9 $\alpha_{CO2/N2}$ = 12.9 $\alpha_{O2/N2}$ = 1.5 P = 155.8	Murali et al. [114]
CO_2/CH_4	PI	SSZ-13	$\alpha_{CO2/CH4}$ = 37.1 P = 57.3	$\alpha_{CO2/CH4}$ = 49.6 P = 67	Hillock et al. [168]

*P is the CO_2 permeability in Barrer; α is the selectivity; 1 GPU = 10^{-6} cm^3 (STP)/cm^2 cmHg s.

agglomerate formation [154]. HZSs have gained attention as a result of combining the exciting characteristics of spherical particles and zeolites. They exhibit high permeability by the nature of hollow spheres, which permit the rapid flow of gas molecules while preserving the selectivity by the zeolite shell molecular sieving effect [213].

The most common preparation processes of HZSs include self-assembly and layer-by-layer (LbL) deposition [212]. In the LbL process, mesoporous silica spheres (MSSs) are first synthesized using the Schulz-Ekloff method [214]. Afterward, the dispersed MSSs in distilled water are placed in contact with a NaCl solution containing poly(diallyldimethylammonium chloride) (PDDA). Then, the PDDA-MSS suspension is mixed with a solution containing small contents of NH_4OH and silicalite-1 seeds. Washing with distilled water followed by centrifugation is used to remove the excess content of silicalite-1. At this point, the MSSs were encapsulated with a monolayer of silicalite-1 by the LbL seeding process. Lastly, silicalite-1 seeded MSSs were produced hydrothermally, where all MSSs were converted into HZSs [213,215].

Zornoza et al. were the first to incorporate HZSs in MMMs fabricated for CO_2 gas separations [213]. The MMMs were synthesized by combining two different polymers (polyimide (Matrimid®), PSF (Udel®)), and hollow silicalite-1 spheres (HZSs) (with ~ 4 μm diameter). The hollow nature of HZSs improved permeability; meanwhile, the spherical shape enhanced the filler dispersion and interfacial adhesions with the polymer matrix. The HZSs were prepared as aforementioned, and it was

Table 4
Summary of gas transport properties of modified zeolite-filled MMMs.

Gas type	Host matrix	Zeolite type	Membrane performance		Ref
			Neat polymeric membrane	Mixed Matrix Membrane	
CO_2/CH_4, CO_2/N_2	PI	4A-TAP	$\alpha_{CO2/CH4} = 1.22$ $\alpha_{CO2/N2} = 3.8$ $P = 8.34$	$\alpha_{CO2/CH4} = 617$ $\alpha_{CO2/N2} = 102$ $P = 0.19$	Yong et al. [163]
CO_2/CH_4	PES	5A/APDEMS, 50 wt%	$\alpha_{CO2/CH4} = 31.6$ $P = 2.6$	$\alpha_{CO2/CH4} = 36.9$ $P = 2.5$	Li et al. [149]
CO_2/CH_4	PES	NaA/Ag^+, 50wt%	$\alpha_{CO2/CH4} = 35.3$ $P = 1$	$\alpha_{CO2/CH4} = 44$ $P = 1.2$	Li et al. [199]
CO_2/CH_4	Matrimid®5218	NaY/Ag^+, 15 wt%	$\alpha_{CO2/CH4} = 36.3$ $P = 8.34$	$\alpha_{CO2/CH4} = 60.1$ $P = 18.62$	Amooghin et al. [200]
CO_2/CH_4	Matrimid®5218	NaY/$[Co(tetra\text{-}aza)]^{2+}$, 15 wt%	$\alpha_{CO2/CH4} = 36.3$ $P = 8.34$	$\alpha_{CO2/CH4} = 111.6$ $P = 18.96$	Amooghin et al. [201]
$CO_2/N_2/CH_4$ 50 psi	PEBA	Na-clinoptilolite/Ca^{2+}	$\alpha_{CO2/CH4} = 5.84$ $\alpha_{N2/CH4} = 0.31$ $P = 479.5$	$\alpha_{CO2/CH4} = 37.36$ $\alpha_{N2/CH4} = 1.67$ $P = 342.9$	Luna et al. [202]
CO_2/CH_4 50 psi	PSF	Clinoptilolite/EA	$\alpha_{CO2/CH4} = 29.38$ $P = 17.34$	$\alpha_{CO2/CH4} = 45.78$ $P = 22.79$	Castruita-de León et al. [203]
CO_2/CH_4	PSF	SAPO-34/HFDS 1.0, 10 wt%	$\alpha_{CO2/CH4} = 17.2$ $P = 21.3$ GPU	$\alpha_{CO2/CH4} = 38.9$ $P = 278.8$ GPU	Junaidi et al. [204]

*P is the CO_2 permeability in Barrer; α is the selectivity; 1 GPU = 10^{-6} cm^3 (STP)/cm^2 cmHg .

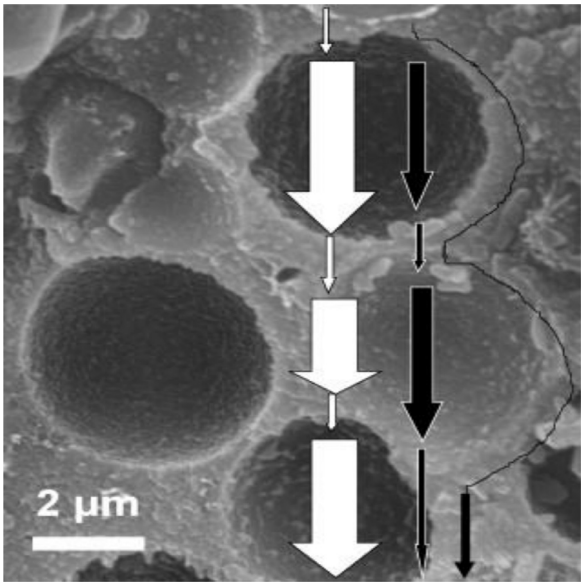

Fig. 12. SEM micrograph of 8 wt% hollow zeolite sphere (HZS)/polysulfone (PSF) membrane. The white arrows describe the transport of faster permeating molecules (such as CO_2) through the PSF and HZS phases, while the black ones demonstrate the transport of the slower permeating molecules (such as N_2). The arrow thickness relates to how fast the gas molecules can transport through the PSF and HZS media [213].

revealed that the membranes with 8 wt% of HZSs displayed better separation factors than those prepared by the neat polymer and conventional silicalite-1 crystals of similar diameter to that of HZSs (Fig. 12). The CO_2/N_2, H_2/CH_4, and O_2/N_2 selectivities reached 41.7, 180, and 8.5, respectively. Fig. 12 shows that selected molecules can permeate more quickly in the hollow filler than those whose adsorption or diffusion is not preferred by zeolites. The same group also compared the impact of HZSs with MCM-41 spheres (MSSs) and Grignard surface-modified MSSs (Mg-MSSs) on the gas separation performance of 6FDA-DAM MMMs [156]. They emphasized that the 8 wt% Mg-MSS/6FDA-DAM membrane was the best performing one with CO_2/N_2, H_2/CH_4, O_2/N_2, and CO_2/CH_4 selectivities of 24.4, 21.8, 4.3, and 31.5, respectively. This improved performance can be linked to the enhanced interfacial adhesions with the polymer networks as a result of the $Mg(OH)_2$ treatment.

3.5.2. Sheet-like particles

High zeolite content is required to improve the gas transport properties of MMMs. They also form thick membranes as a result of their normal micron-size [216]. Thus, to overcome these limitations, porous layered fillers have been designed. Sheet-like fillers offer a longer tortuous path for larger molecules and hence decrease their permeability [217]. Interestingly, layered fillers can be exfoliated or delaminated into single- or few-layered nano-structures, which can exhibit a larger adsorption surface area, higher permeability, and lower diffusion resistance for smaller molecules [218]. Different nanoporous layered materials, including AMH-3 and Jilin-Davy-Faraday, layered solid No. 1 (JDF-L1) have been used [143] and will later be discussed in the proceeding sections.

AMH-3 layered silicates: AMH-3 are 3D porous layered silicates comprised of eight-membered-ring pores [219]. The internal porosity of AMH-3 is reachable from all directions [220]. The pore size of AMH-3 is 3.4 Å [221], which makes it a promising candidate in CO_2/CH_4 and H_2/CO_2 separations [218]. Besides, AMH-3 particles have charge-balancing cations in the interlayer spaces and silanol groups on the surface [222]. AMH-3 silicate layers can be exfoliated via swelling of the interlayer space while maintaining the pore structure [222]. For instance, sequential intercalation of dodecylamine following proton-exchange (herein referred to as H-exchange) in the presence of DL-histidine was achieved by Choi et al. to swell AMH-3 silicates [223,224]. The H_2/CO_2 ideal selectivity of polybenzimidazole (PBI) membranes was increased from 15 for the neat PBI membrane to 40 after incorporating only 3 wt% of swollen AMH-3 [224]. This enhancement is possibly due to the silicate's molecular sieving behavior. Moreover, the swollen AMH-3 MMMs displayed a noteworthy decline in CO_2 permeability. Fig. 13a demonstrates the SEM micrograph of the H-exchanged AMH-3 particles; these particles were precipitated in the bottom side of the membranes (Fig. 13b). Fig. 13c showed the loss of well-defined compact shape after swelling the H-exchanged particles. Mixing the swollen particles with PBI (Fig. 13d) resulted in a new MMM. From Fig. 13e, the power-law q-dependence of the membrane with 3 wt% of H-exchanged AMH-3 ($\sim q^{-2.1}$) observed in the low-q region is close to the theoretical value for disk-like particles (q^{-2}) [225–227]. The broad peak seen at q=0.9 nm^{-1} realized the non-completed exfoliation process. TEM and SAXS results revealed the nanocomposites exist as thin platelets [217].

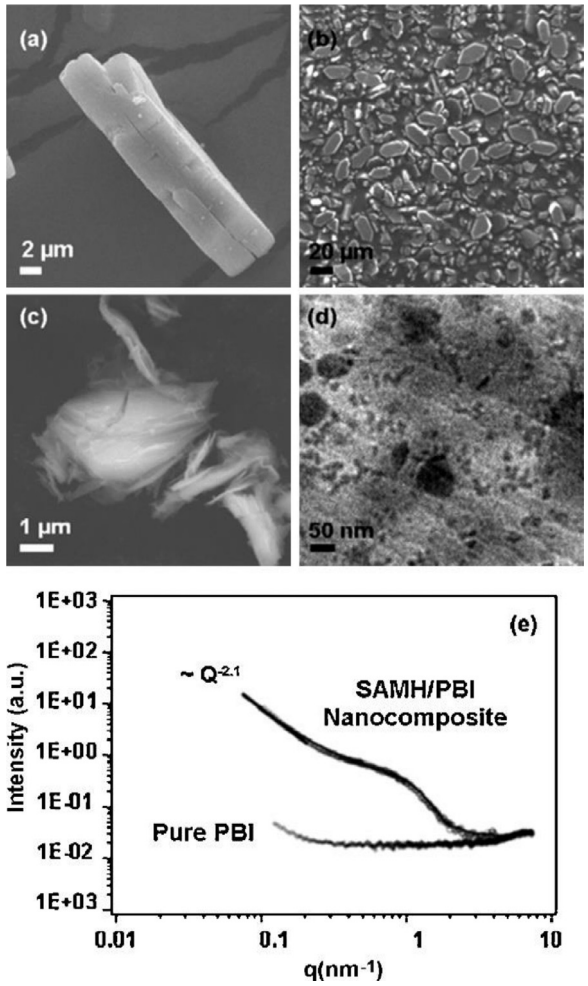

Fig. 13. (a) SEM micrograph of H-exchanged AMH-3; (b) SEM micrograph of H-exchanged AMH-3 (14 wt%)/polybenzimidazole (PBI) membrane; (c) SEM micrograph of swollen AMH-3; (d) TEM image of swollen AMH-3 (3 wt%)/PBI membrane; and (e) corresponding SAXS pattern [224].

In another study, Kim et al. [222] increased the CO_2 permeability by 54% with a minor improvement in CO_2/CH_4 selectivity after adding 6 wt% of dodecylamine-swollen AMH-3 particles into a cellulose acetate (CA) membrane. They delaminated AMH-3 into flakes using a high shear mixer. The gas transport properties got improved due to the pores molecular sieving behavior. Results recommended using a high-viscousity polymer solution instead of water for vortex mixing to achieve better exfoliation that might occur as a result of increasing the shear stress on the sheets, which determine the exfoliation degree. Conventional dispersion techniques, including stirring and sonication, cannot guarantee highquality exfoliation of swollen AMH-3 layers in the polymer matrix [222]. AMH-3 silicates are hydrophilic due to the existence of cations between the silicate layers. Thus, to overcome the dispersion limitations, surface modification of AMH-3 demonstrates a potential approach to improve its compatibility with hydrophobic polymers. In this context, Tzi et al. functionalized swollen AMH-3 layered silicate with octyl(methyl)dimethoxysilane to improve its hydrophobicity, thereby developing dispersion and adhesion with PSF matrix [228]. The functionalization process reduced the pore size and increased surface area. The fabricated MMMs displayed excellent dispersion and distribution of swollen AMH-3 particles in the polymer matrix. Therefore, the introduction of functionalized AMH-3 layers into the PSF matrix can improve the gas separation characteristics of the MMMs. Because of the swelling method difficulty, incorporating swollen AMH-3 particles into MMMs for CO_2/CH_4 separations is still limited and needs to be further investigated [218].

JDF-L1 titanosilicates: Similar to zeolites, titanosilicates exhibit microporous crystalline morphology comprised of 3D frameworks with channels and cavities. The difference is that the zeolite frameworks mainly consist of AlO_4- and SiO_4-tetrahedra, whereas titanosilicate frameworks consist of SiO_4-tetrahedra and TiO_5-pentahedra or TiO_6-octahedra. Titanosilicates offer excellent cation-exchange (such as Ti-replacement) and high specific surface area [216,222,229].

JDF-L1 (known as Na-titanosilicate (NTS) [230] and Aveiro-Manchester 1 (AM-1) [231]) is a sheet-like microporous titanosilicate with a pore size of 3 Å [232]. It consists of TiO_5-square pyramids in which each vertex of the base is connected to SiO_4-tetrahedra to constitute continuous sheets of $TiO.O_4(SiO_3)_4$ with exchangeable interlamellar Na^+ ions [233]. One TiO_5-square pyramid and four SiO_4-tetrahedra shape pore along with the layers orientation in <010> and <100> directions. Besides, six-membered rings of two TiO_5-square pyramids and four SiO_4-tetrahedra create another set of pores across the layers along <001> direction. Two interlamellar H_2O molecules coordinate the Na^+ ions placed at the center in front of the pores in <001> direction, and two layers of Na^+ ions sandwich one layer of H_2O molecules [232,234–236].

Based on the size-exclusion characteristics, JDF-L1 layers consist of six-membered rings that can improve the selectivity for small molecules. This property makes it a potential applicant for CO_2/CH_4 separations [103,237]. The orientation of its layers in the polymer matrix mainly determines the gas transport properties of MMMs [103]. In other words, the horizontal orientation substantially enhances the gas separation performance as compared to the random orientation. Moreover, swollen JDF-L1 (also known as UZAR-S1) can be prepared by exfoliating the JDF-L1 titanosilicate [238]. The exfoliation technique can be established by intercalating JDF-L1 with alkylamines via hydrogen bonding with interlayer groups or ion-exchange processes [234]. UZAR-S1 layers are non-agglomerated sheet-like ones with thicknesses of ~ 100 nm and high area/volume aspect ratios [238]. However, the incorporation of JDF-L1 and UZAR-S1 in a polymer matrix for CO_2/CH_4 separations is still limited [103,232,235].

For H_2/CH_4 separations, Rubio et al. [238] reported the exfoliation of JDF-L1 titanosilicate to synthesize UZAR-S1. They first H-exchanged the JDF-L1 particles with histidine and then did intercalation with nonyl amine and final extraction in a solution of H_2O/HCl/ethanol. The dispersion of 4 wt% of UZAR-S1 layers in the PSF matrix resulted in an enhanced H_2/CH_4 selectivity (69.2) compared with the pure PSF membrane (58.9). Furthermore, Castarlenas et al. exfoliated the swollen JDF-L1 through a melt compounding method to prepare PSF membranes incorporated with JDF-L1 nanoplatelets [234]. The MMMs demonstrated an enhanced separation performance compared with the chemically exfoliated JDF-L1/PSF or with neat PSF membranes. The best separation performance corresponded to an 8.3 wt% MMM with H_2/CH_4 selectivity and H_2 permeability of 128 and 12.5 Barrer, respectively. The improved separation performance was attributed to the excellent dispersion of exfoliated JDF-L1 particles with pores inaccessible to CH_4 molecules (~ 3 Å). It was also revealed that increasing an exfoliation extent can further enhance the gas separation behavior of the synthesized MMMs. Interestingly, Galve et al. [235] combined the spherical ordered mesoporous silica MCM-41 with layered microporous JDF-L1 for preparing copolyimide 6FDA-4MPD/6FDA-DABA MMMs. The separation performance was improved by combining highly permeable inorganic spheres (MCM-41) and highly selective inorganic sheets (JDF-L1). The MMM contained 4 wt% of JDF-L1 and 8 wt% of MCM-41 displayed H_2 permeability of 440 Barrer with H_2/CH_4 selectivity of 32.0.

3.5.3. Zeolitic imidazolate frameworks (ZIFs)

MOFs are widely applied in MMMs fabrication due to their attractive characteristics such as high adsorption capacity, tunable pore structure, high surface area, and excellent thermal and chemical properties. The

Table 5
Summary of gas separation factors of zeolite-like filled MMMs.

Gas type	Host matrix	Zeolite-like type	Membrane performance		Ref
			Neat polymeric membrane	Mixed Matrix Membrane	
H_2/CH_4, CO_2/N_2, O_2/N_2	Udel®	HZS, 8 wt%	$\alpha_{H2/CH4}=58.9$ $\alpha_{CO2/N2}=24.3$ $\alpha_{O2/N2}=4.7$ $P=5.9$	$\alpha_{H2/CH4}=80.3$ $\alpha_{CO2/N2}=41.7$ $\alpha_{O2/N2}=6.9$ $P=7.2$	Zornoza et al. [213]
	Matrimid®	HZS, 8 wt%	$\alpha_{H2/CH4}=132$ $\alpha_{CO2/N2}=26.6$ $\alpha_{O2/N2}=5.5$ $P=7.6$	$\alpha_{H2/CH4}=180$ $\alpha_{CO2/N2}=39.8$ $\alpha_{O2/N2}=8.5$ $P=18.7$	
H_2/CH_4, CO_2/N_2, O_2/N_2, CO_2/CH_4	6FDA-DAM	HZS, 8 wt%	$\alpha_{H2/CH4}=16.5$ $\alpha_{CO2/N2}=16.5$ $\alpha_{O2/N2}=3.3$ $\alpha_{CO2/CH4}=21.4$ $P_{CO2/CH4}=681$	$\alpha_{H2/CH4}=25.4$ $\alpha_{CO2/N2}=27.1$ $\alpha_{O2/N2}=4.4$ $\alpha_{CO2/CH4}=31.1$ $P_{CO2/CH4}=712$	Zornoza et al. [156]
H_2/CO_2	PBI	Swollen AMH-3, 3 wt%	$\alpha_{H2/CO2}=15$	$\alpha_{H2/CO2}=40$	Choi et al. [224]
CO_2/CH_4	CA	Swollen AMH-3, 6 wt%	$\alpha_{CO2/CH4}=29.61$ $P=7.55$	$\alpha_{CO2/CH4}=29.71$ $P=11.59$	Kim et al. [222]
H_2/CH_4	PSF	UZAR-S1, 4 wt%	$\alpha_{H2/CH4}=58.9$ $P_{H2}=11.8$	$\alpha_{H2/CH4}=69.2$ $P_{H2}=11.5$	Rubio et al. [238]
H_2/CH_4	PSF	Swollen JDF-L1, 8.3 wt%	$\alpha_{H2/CH4}=58.9$ $P_{H2}=11.8$	$\alpha_{H2/CH4}=128$ $P_{H2}=12.5$	Castarlenas et al. [234]
H_2/CH_4, O_2/N_2	6FDA-4MPD/6FDA-DABA	JDF-L1, 4 wt% and MCM-41, 8 wt%	$\alpha_{H2/CH4}=18.9$ $\alpha_{O2/N2}=4.1$ $P_{H2}=311$	$\alpha_{H2/CH4}=32.0$ $\alpha_{O2/N2}=3.6$ $P_{H2}=440$	Galve et al. [235]
CO_2/N_2	Pebax®2533	ZIF-7-OH, 14 wt%	$\alpha_{CO2/N2}=15.5$ $P=171$	$\alpha_{CO2/N2}=38$ $P=273$	Gao et al. [241]
CO_2/CH_4, 4 bar	PU	ZIF-8, 30 wt%	$\alpha_{CO2/CH4}=7.5$ $P=2.7$	$\alpha_{CO2/CH4}=13.7$ $P=14.2$	Gholami et al. [242]
$He/H_2/O_2/N_2/CH_4/CO_2$	HPI, TR-90	ZIF-8, 20 wt%	$\alpha_{H2/CH4}=80.6$ $\alpha_{H2/N2}=42.7$ $\alpha_{CO2/CH4}=50.5$ $P_{H2}=186$ $P=117$	$\alpha_{H2/CH4}=27.9$ $\alpha_{H2/N2}=21.3$ $\alpha_{CO2/CH4}=21.9$ $P_{H2}=1206$ $P=947$	Kim et al. [243]
$CO_2/CH_4/N_2$	PSF	ZIF-8, 5 wt%/GO, 5wt%	$\alpha_{CO2/CH4}=3.9$ $\alpha_{CO2/N2}=0.8$ $P=0.94$	$\alpha_{CO2/CH4}=6.3$ $\alpha_{CO2/N2}=4.9$ $P=1.76$	Anastasiou et al. [244]
CO_2/N_2	6FDA-DAM	ZIF-94, 40 wt%	$\alpha_{CO2/N2}=24$ $P=770$	$\alpha_{CO2/N2}=22$ $P=2310$	Etxeberria-Benavides et al. [125]

*P is the CO_2 permeability in Barrer; α is the selectivity.

presence of organic moiety in MOFs adds to the development of adhesion interactions between MOF particles and a polymer matrix. ZIFs are a subfamily of MOFs with zeolitic structure and an easily tailorable pore aperture. ZIFs are comprised of transition metal-centered complexes with imidazolate ligands, altogether referred to as secondary building units (SBUs). These SBUs can replace the Si/Al repeating units in zeolites under appropriate conditions. The bond angle between ZIF SBUs (M-imidazolate-M) is ~145°, comparable to that in aluminosilicate zeolites [239]. ZIFs have large cavities with narrow pore apertures close to the kinetic diameter of CO_2 (3.3 Å), and this makes them a potential filler in MMMs fabrication for advanced CO_2 removal. The transition metals (cobalt or zinc) and organic linkers of imidazolate ligands can be varied to synthesize a series of ZIF structures such as ZIF-7, ZIF-8, ZIF-11, ZIF-78, ZIF-94, and ZIF-302. Here we will discuss the influence of various ZIFs on the gas separation performance of MMMs.

A small change in the structure of MMMs can extensively affect the separation performance of the synthesized MMMs. For clarifying, Azizi et al. [240] added different amounts of ZIF-7 nanoparticles to a Pebax-1074 matrix to enhance CO_2/CH_4 separation. They synthesized ZIF-7 using benzimidazole and zinc nitrate hexahydrate. The CO_2/CH_4 selectivity and CO_2 and CH_4 permeabilities increased with increasing ZIF-7 nanoparticle content up to 10 wt%. With a further increment in the ZIF-7 content, the CO_2/CH_4 selectivity increased, due to the molecular sieving property of the ZIF-7 nanoparticles, while CO_2 and CH_4 permeabilities declined due to the presence of rigidified polymer chains. The best CO_2/CH_4 separation performance was obtained in 25 wt% MMM with CO_2/CH_4 selectivity of 28.09 (increased from 20.38 for the neat polymer membrane, ~ 38% increment). Recently, Gao et al. functionalized ZIF-7 frameworks with three different functional groups (OH, CH_3OH, and NH_2) and incorporated these frameworks into the Pebax®2533 matrix [241]. Incorporating functional groups into ZIF-7 structures is indeed beneficial for the CO_2 capture process. All membranes consisting of functionalized ZIF-7 frameworks displayed higher CO_2/N_2 selectivity than unmodified ZIF-7/Pebax®2533 MMM. Among the three modified ZIF-7 MMMs, the OH-modified ZIF-7/Pebax®2533 membrane offered the best CO_2/N_2 separation performance, which may be credited to the highest CO_2/N_2 adsorption selectivity. By adding 14 wt% of OH-functionalized ZIF-7 particles, the CO_2 permeability and CO_2/N_2 selectivity were increased to 273 Barrer (60% increment) and 38 (145% increment), respectively.

For another exciting member of the ZIF series, Gholami et al. impregnated the PU matrix with ZIF-8 nanoparticles prepared using zinc nitrate hexahydrate and 2-methylimidazole [242]. Adding ZIF-8 nanoparticles to the PU matrix enhanced the thermal stability of the networks. The CO_2 and CH_4 permeabilities were enhanced by increasing the ZIF-8 nanoparticles loading, due to the increased free volume, and the CO_2/CH_4 selectivity was also enhanced. With introducing 30 wt% of ZIF-8 nanoparticles, the CO_2/CH_4 selectivity and CO_2 permeability were improved by 83% and 426%, respectively. The gas transport measurements were conducted at different feed pressures (4, 8, and 12 bar), and the gas transport properties were substantially enhanced by increasing the feed pressure. For H_2/CH_4 separations, MMMs with thermally rearranged (TR) hydroxyl polyimide (HPI) and ZIF-8 crystals were recently designed by Kim et al. [243]. The HPI membranes were thermally

treated under an inert gas atmosphere to produce TR membranes. During the TR process, the interfacial voids between ZIF-8 particles and TR polymer, which commonly arise in most MMMs, were alleviated. The TR procedure can tune the cavity size and consequently determine the gas transport factors of the designed MMMs. ZIF-8 frameworks enhanced the gas permeability and also controlled the thermal conversion % of the TR polymer. By adding 20 wt% of ZIF-8 crystals and achieving 90% TR conversion (TR-90-ZIF8-20 membrane), the H_2 and CO_2 permeabilities achieved 1206 and 947 Barrer, respectively, whereas the H_2/CH_4, H_2/N_2, and CO_2/CH_4 selectivities were 27.9, 21.3, and 21.9, respectively. Combining two or more fillers functionality represents a promising approach to boost the gas separation behavior of MMMs. In this context, Anastasiou et al. [244] incorporated ZIF-8/graphene oxide (GO) hybrid nanofillers into the PSF network. The ZIF-8/GO/PSF membranes improved the CO_2 permeability by up to 87% and CO_2/CH_4 selectivity by up to 61%, whereas the N_2 permeability was significantly declined. Moreover, the CO_2/CH_4 selectivity for ZIF-8/GO/PSF membrane was improved by up to an enhancement of 7-fold compared with the ZIF-8/PSF membrane. This influence can be attributed to GO particles higher affinity towards CO_2 molecules compared to other gases [245]. Namely, the π-π bond of GO interacts strongly with polar CO_2 molecules, and also GO particles form interfacial voids, which increase the free volume and hence improve the CO_2 permeability [246]. In addition, the polar functional groups of GO, such as carboxyl and hydroxyl groups, react with the polar CO_2 gas more than the non-polar gases [247,248].

Etxeberria-Benavides et al. [125] recently synthesized novel ZIF-94 crystals (with particle size < 500 nm) using methanol and tetrahydrofuran (nonhazardous solvent) instead of N,N-dimethylformamide (DMF) (hazardous solvent), and then incorporated them into 6FDA-DAM matrix. The CO_2 permeability improved at the same CO_2/N_2 selectivity of 22. The highest CO_2 permeability reached 2310 Barrer (~ 200% increment), with adding 40 wt% of ZIF-94 crystals. Additionally, Cacho-Bailo et al. imine-functionalized ZIF-94 frameworks using a microfluidic approach for developing P84® membranes [249]. The post-imine modification using hexyl- and nonylamine resulted in improving CO_2 permeability while maintaining an excellent selectivity-permeability balance. The imine modification is theorized to have rearranged the ZIF-94 frameworks in a less dense morphology (higher free volume) with a larger pore size and a reduced CO_2 affinity. The MMMs offered CO_2/CH_4, H_2/CH_4, and He/CH_4 selectivities of 27.8, 85.6, and 79.1, respectively. Table 5 summarizes the gas transport factors of zeolite-like filled MMMs.

4. Conclusion and future prospects

To reduce greenhouse emissions, it is essential to separate CO_2 from a flue or exhaust gas that emanates from combustion plants. In this context, zeolites are widely used in CO_2 adsorption and MMMs due to their tailorable cavities and pore sizes, high surface area, hydrothermal stability, low-cost, and high accessibility. The literature contributions have established the aptitudes of chemically modified zeolites to improve CO_2 adsorption behavior via amine, silica, and ion-exchange treatments. Moreover, the main effect of reducing zeolite particle size from micrometers to nanometers when they are used as adsorbents appears in improvement of diffusion characteristics and adsorption capacities. Hybrid foams using meso/macroporous supporting materials can be designed to sustain ultra-high contents of zeolites without the necessity of adding crosslinkers. Improving compatibility and interfacial adhesions between filler and polymer matrices to overcome the trade-off between gas selectivity and permeability faced by pure polymeric membranes, results in suppressing the interfacial voids and improving the gas transport properties. Thus, it is vital to accept an appropriate approach to exploiting the modified zeolites beneficial properties and zeolite-like structures to fabricate MMMs with improved gas transport properties.

Dual chemical modification of zeolites offers an interesting potential of further improvement of the CO_2 separation performance and subsequently must gain more attention in the years to come. Using nano-size fillers is an emerging new strategy to drastically increase the particulate-matrix contact area and the interfacial adhesion. Thus, fabrication of the next generation of MMMs will be employing novel zeolite nanostructures, i.e. nanospheres, nanofibers, and nanoplatelets, averting the filler agglomerations and guaranteeing a full exploitation of their gas transport properties. Moreover, zeolite-like layered fillers can be exfoliated into single- or few-layered nano-structures to further improve the gas separation performance. The future research efforts must also be directed towards developing hybrid nanocomposites combining zeolites with other filler, i.e. graphene oxide to enhance CO_2 separation performance and attain other novel material characteristics. Finally, we hope the present review provides a spirit about zeolite and zeolite-like materials as adsorbents and fillers for MMMs, which could be a beacon for researchers in this field.

Declaration of Competing Interest

The authors declare that they have no known competing financial interests or personal relationships that could have appeared to influence the work reported in this paper.

Acknowledgments

This publication was made possible by the NPRP Grant # NPRP10-0126-170257 from the Qatar National Research Fund (a member of the Qatar Foundation). The statements made herein are solely the responsibility of the authors.

References

[1] G. Busca, Zeolites and other structurally microporous solids as acid–base materials, in: G. Busca (Ed.), Heterog. Catal. Mater., Elsevier, Amsterdam, 2014, pp. 197–249. http://www.sciencedirect.com/science/article/pii/B9780444595249000079.
[2] J.D. Sherman, Synthetic zeolites and other microporous oxide molecular sieves, Proc. Natl. Acad. Sci. 96 (1999) 3471–3478 http://www.pnas.org/content/96/7/3471.abstract.
[3] M. Tagliabue, D. Farrusseng, S. Valencia, S. Aguado, U. Ravon, C. Rizzo, A. Corma, C. Mirodatos, Natural gas treating by selective adsorption: Material science and chemical engineering interplay, Chem. Eng. J. 155 (2009) 553–566 http://www.sciencedirect.com/science/article/pii/S1385894709006111.
[4] D. Panda, E.A. Kumar, S.K. Singh, Amine modification of binder-containing zeolite 4A bodies for post-combustion CO_2 capture, Ind. Eng. Chem. Res. 58 (2019) 5301–5313 10.1021/acs.iecr.8b03958.
[5] J.-L. Paillaud, B. Harbuzaru, J. Patarin, N. Bats, Extra-large-pore zeolites with two-dimensional channels formed by 14 and 12 rings, Science (80-.) 304 (2004) 990 LP – 992 10.1126/science.1098242 .
[6] J.M. Castillo, J. Silvestre-Albero, F. Rodriguez-Reinoso, T.J.H. Vlugt, S. Calero, Water adsorption in hydrophilic zeolites: experiment and simulation, Phys. Chem. Chem. Phys. 15 (2013) 17374–17382 10.1039/C3CP52910J.
[7] J. Weitkamp, L. Puppe (Eds.), Catalysis and Zeolites – Fundamentals and Applications, Springer, 1999.
[8] H. Qu, Y. Ma, B. Li, L. Wang, Hierarchical zeolites: synthesis, structural control, and catalytic applications, Emergent Mater. 3 (2020) 225–245 10.1007/s42247-020-00088-z.
[9] C.-Y. Chen, S.I. Zones, Post-synthetic treatment and modification of zeolites, Zeolites Catal (2010) 155–170 10.1002/9783527630295.ch6.
[10] A.W. Burton, S.I. Zones, S. Elomari, The chemistry of phase selectivity in the synthesis of high-silica zeolites, Curr. Opin. Colloid Interface Sci. 10 (2005) 211–219 http://www.sciencedirect.com/science/article/pii/S1359029405000579.
[11] M.A. Camblor, L.A. Villaescusa, M.J. Díaz-Cabañas, Synthesis of all-silica and high-silica molecular sieves in fluoride media, Top. Catal. 9 (1999) 59–76 10.1023/A:1019154304344.
[12] A. Corma, M.E. Davis, Issues in the synthesis of crystalline molecular sieves: towards the crystallization of low framework-density structures, ChemPhysChem 5 (2004) 304–313 10.1002/cphc.200300997.
[13] G.S. Lee, Y. Nakagawa, S.-J. Hwang, M.E. Davis, P. Wagner, L. Beck, S.I. Zones, Organocations in zeolite synthesis: fused bicyclo [l.m.0] cations and the discovery of zeolite SSZ-48, J. Am. Chem. Soc. 124 (2002) 7024–7034 10.1021/ja011513o.
[14] R.F. Lobo, S.I. Zones, M.E. Davis, Structure-direction in zeolite synthesis, J. Incl. Phenom. Mol. Recognit. Chem. 21 (1995) 47–78 10.1007/BF00709411.
[15] R. Millini, G. Perego, G. Bellussi, Synthesis and characterization of boron-containing molecular sieves, Top. Catal. 9 (1999) 13–34 10.1023/A:1019198119365.

[16] Y. Nakagawa, G.S. Lee, T.V Harris, L.T. Yuen, S.I. Zones, Guest/host relationships in zeolite synthesis: ring-substituted piperidines and the remarkable adamantane mimicry by 1-azonio spiro [5.5] undecanes1Dedicated to Professor Lovat V.C. Rees in recognition and appreciation of his lifelong devotion to zeolite, Microporous Mesoporous Mater. 22 (1998) 69–85 http://www.sciencedirect.com/science/article/pii/S1387181198001061.

[17] S.I. Zones, S.-J. Hwang, The inorganic chemistry of guest-mediated zeolite crystallization: a comparison of the use of boron and aluminum as lattice-substituting components in the presence of a single guest molecule during zeolite synthesis, Microporous Mesoporous Mater. 58 (2003) 263–277 http://www.sciencedirect.com/science/article/pii/S1387181102006534.

[18] S.I. Zones, Y. Nakagawa, G.S. Lee, C.Y. Chen, L.T. Yuen, Searching for new high silica zeolites through a synergy of organic templates and novel inorganic conditions, Microporous Mesoporous Mater 21 (1998) 199–211 http://www.sciencedirect.com/science/article/pii/S1387181198000110.

[19] S.I. Zones, M.E. Davis, Zeolite materials: recent discoveries and future prospects, Curr. Opin. Solid State Mater. Sci. 1 (1996) 107–117 http://www.sciencedirect.com/science/article/pii/S1359028696800180.

[20] S.I. Zones, Y. Nakagawa, Boron-beta zeolite hydrothermal conversions: the influence of template structure and of boron concentration and source, Microporous Mater 2 (1994) 543–555 http://www.sciencedirect.com/science/article/pii/0927651394000255.

[21] R. Szostak, Secondary synthesis methods, in: H. van Bekkum, E.M. Flanigen, P.A. Jacobs, J.C. Jansen (Eds.), Introduction to Zeolite Science and Practice, 2nd ed., Elsevier, 2001, pp. 261–297. http://www.sciencedirect.com/science/article/pii/S0167299101802482.

[22] G.H. Kühl, Modification of zeolites, in: J. Weitkamp, L. Puppe (Eds.), Catal. Zeolites – Fundam. Appl., Springer, 1999, pp. 81–197.

[23] D. Bastani, N. Esmaeili, M. Asadollahi, Polymeric mixed matrix membranes containing zeolites as a filler for gas separation applications: a review, J. Ind. Eng. Chem. 19 (2013) 375–393 10.1016/j.jiec.2012.09.019.

[24] Y. Li, L. Li, J. Yu, Applications of zeolites in sustainable chemistry, Chem 3 (2017) 928–949 10.1016/j.chempr.2017.10.009.

[25] P.A. Webley, Adsorption technology for CO_2 separation and capture: a perspective, Adsorption 20 (2014) 225–231 10.1007/s10450-014-9603-2.

[26] S. Choi, J.H. Drese, C.W. Jones, Adsorbent materials for carbon dioxide capture from large anthropogenic point sources, ChemSusChem 2 (2009) 796–854 10.1002/cssc.200900036.

[27] D.Y.C. Leung, G. Caramanna, M.M. Maroto-Valer, An overview of current status of carbon dioxide capture and storage technologies, Renew. Sustain. Energy Rev. 39 (2014) 426–443 10.1016/j.rser.2014.07.093.

[28] N. Hedin, L. Chen, A. Laaksonen, Sorbents for CO2 capture from flue gas—aspects from materials and theoretical chemistry, Nanoscale 2 (2010) 1819–1841 10.1039/C0NR00042F.

[29] C.-H. H. Yu Chih-Hung, Chung-Sung Tan, A review of CO_2 capture by absorption and adsorption, Aerosol. Air Qual. Res. 12 (2012) 745–769 10.4209/aaqr.2012.05.0132 .

[30] R.T. Yang, Adsorbents: Fundamentals and Applications, Wiley, New York, 2003 10.1002/047144409X.

[31] X. Liu, F. Gao, J. Xu, L. Zhou, H. Liu, J. Hu, Zeolite@Mesoporous silica-supported-amine hybrids for the capture of CO_2 in the presence of water, Microporous Mesoporous Mater. 222 (2016) 113–119 http://www.sciencedirect.com/science/article/pii/S138718111500551X.

[32] Q. Liu, T. Pham, M.D. Porosoff, R.F. Lobo, ZK-5: A CO_2-selective zeolite with high working capacity at ambient temperature and pressure, ChemSusChem 5 (2012) 2237–2242 10.1002/cssc.201200339.

[33] F. Akhtar, Q. Liu, N. Hedin, L. Bergström, Strong and binder free structured zeolite sorbents with very high CO_2-over-N_2 selectivities and high capacities to adsorb CO_2 rapidly, Energy Environ. Sci. 5 (2012) 7664–7673 10.1039/C2EE21153J.

[34] Q. Liu, A. Mace, Z. Bacsik, J. Sun, A. Laaksonen, N. Hedin, NaKA sorbents with high CO_2-over-N_2 selectivity and high capacity to adsorb CO_2, Chem. Commun. 46 (2010) 4502–4504 10.1039/C000900H.

[35] F. Akhtar, S. Ogunwumi, L. Bergström, Thin zeolite laminates for rapid and energy-efficient carbon capture, Sci. Rep. 7 (2017) 10988 10.1038/s41598-017-10518-4.

[36] D.W. Breck, Zeolite Molecular Sieves: Structure, Chemistry, and Use, Wiley, New York, 1973.

[37] M. Niwa, S. Kato, T. Hattori, Y. Murakami, Fine control of the pore-opening size of the zeolite mordenite by chemical vapour deposition of silicon alkoxide, J. Chem. Soc. Faraday Trans. 1 Phys. Chem. Condens. Phases. 80 (1984) 3135–3145 10.1039/F19848003135.

[38] S.M. Kuznicki, V.A. Bell, S. Nair, H.W. Hillhouse, R.M. Jacubinas, C.M. Braunbarth, B.H. Toby, M. Tsapatsis, A titanosilicate molecular sieve with adjustable pores for size-selective adsorption of molecules, Nature 412 (2001) 720–724 10.1038/35089052.

[39] Z. Song, Y. Huang, W.L. Xu, L. Wang, Y. Bao, S. Li, M. Yu, Continuously adjustable, molecular-sieving “Gate” on 5A zeolite for distinguishing small organic molecules by size, Sci. Rep. 5 (2015) 13981 10.1038/srep13981.

[40] Y. Zhao, B. Shen, H. Sun, Chemical liquid deposition modified ZSM-5 zeolite for adsorption removal of dimethyl disulfide, Ind. Eng. Chem. Res. 55 (2016) 6475–6480 10.1021/acs.iecr.5b04902.

[41] D.K.J.A. Wanigarathna, B. Liu, J. Gao, Adsorption separation of R134a, R125, and R143a fluorocarbon mixtures using 13X and surface modified 5A zeolites, AIChE J. 64 (2018) 640–648 10.1002/aic.15955.

[42] L.A. Darunte, K.S. Walton, D.S. Sholl, C.W. Jones, CO2 capture via adsorption in amine-functionalized sorbents, Curr. Opin. Chem. Eng. 12 (2016) 82–90 10.1016/j.coche.2016.03.002.

[43] P.J.E. Harlick, F.H. Tezel, An experimental adsorbent screening study for CO_2 removal from N_2, Microporous Mesoporous Mater 76 (2004) 71–79 10.1016/j.micromeso.2004.07.035.

[44] S. Cavenati, C.A. Grande, A.E. Rodrigues, Upgrade of Methane from Landfill Gas by pressure swing adsorption, Energy Fuels 19 (2005) 2545–2555 10.1021/ef050072h.

[45] D.P. Bezerra, F.W.M. da Silva, P.A.S. de Moura, A.G.S. Sousa, R.S. Vieira, E. Rodriguez-Castellon, D.C.S. Azevedo, CO_2 adsorption in amine-grafted zeolite 13X, Appl. Surf. Sci. 314 (2014) 314–321 10.1016/j.apsusc.2014.06.164.

[46] X. Ma, X. Wang, C. Song, Molecular Basket” Sorbents for Separation of CO_2 and H_2S from various gas streams, J. Am. Chem. Soc. 131 (2009) 5777–5783 10.1021/ja8074105.

[47] D.A. Kennedy, M. Mujčin, C. Abou-Zeid, F.H. Tezel, Cation exchange modification of clinoptilolite –thermodynamic effects on adsorption separations of carbon dioxide, methane, and nitrogen, Microporous Mesoporous Mater. 274 (2019) 327–341 10.1016/j.micromeso.2018.08.035.

[48] P.A.S. Moura, D.P. Bezerra, E. Vilarrasa-Garcia, M. Bastos-Neto, D.C.S. Azevedo, Adsorption equilibria of CO_2 and CH_4 in cation-exchanged zeolites 13X, Adsorption 22 (2016) 71–80 10.1007/s10450-015-9738-9.

[49] J.R. Karra, B.E. Grabicka, Y.-G. Huang, K.S. Walton, Adsorption study of CO_2, CH_4, N_2, and H_2O on an interwoven copper carboxylate metal–organic framework (MOF-14), J. Colloid Interface Sci. 392 (2013) 331–336 10.1016/j.jcis.2012.10.018.

[50] H. Jasuja, K.S. Walton, Experimental study of CO_2, CH_4, and water vapor adsorption on a dimethyl-functionalized UiO-66 framework, J. Phys. Chem. C. 117 (2013) 7062–7068 10.1021/jp311857e.

[51] P.D. Jadhav, R.V Chatti, R.B. Biniwale, N.K. Labhsetwar, S. Devotta, S.S. Rayalu, Monoethanol amine modified zeolite 13X for CO_2 adsorption at different temperatures, Energy & Fuels 21 (2007) 3555–3559 10.1021/ef070038y.

[52] C. Perinu, B. Arstad, A.M. Bouzga, K.-J. Jens, 13C and 15N NMR characterization of amine reactivity and solvent effects in CO_2 capture, J. Phys. Chem. B. 118 (2014) 10167–10174 10.1021/jp503421x.

[53] F. Su, C. Lu, S.-C. Kuo, W. Zeng, Adsorption of CO2 on Amine-Functionalized Y-Type Zeolites, Energy & Fuels 24 (2010) 1441–1448 10.1021/ef901077k.

[54] C.F. Cogswell, Z. Xie, A. Wolek, Y. Wang, A. Stavola, M. Finkenaur, E. Gilmore, M. Lanzillotti, S. Choi, Pore structure–CO_2 adsorption property relations of supported amine materials with multi-pore networks, J. Mater. Chem. A. 5 (2017) 8526–8536 10.1039/C7TA01616F.

[55] F.A. Da Silva, A.E. Rodrigues, Adsorption equilibria and kinetics for propylene and propane over 13X and 4A Zeolite pellets, Ind. Eng. Chem. Res. 38 (1999) 2051–2057 10.1021/ie980640z.

[56] A.K. Ghosh, G. Curthoys, Characterization of zeolite acidity. A gas-chromatographic study using n-butylamine and ammonia, J. Chem. Soc. Faraday Trans. 1 Phys. Chem. Condens. Phases. 79 (1983) 2569–2572 10.1039/F19837902569.

[57] D.P. Bezerra, R.S. Oliveira, R.S. Vieira, C.L. Cavalcante, D.C.S. Azevedo, Adsorption of CO_2 on nitrogen-enriched activated carbon and zeolite 13X, Adsorption 17 (2011) 235–246 10.1007/s10450-011-9320-z.

[58] S. Sircar, A. Myers, Gas Separation by Zeolites, in: S.M. Aurbach, K.A. Carrado, P.K. Dutta (Eds.), Handbook of Zeolite Science and Technology, Dekker, New York, 2003 10.1201/9780203911167.ch22.

[59] X. Xu, X. Zhao, L. Sun, X. Liu, Adsorption separation of carbon dioxide, methane and nitrogen on monoethanol amine modified β-zeolite, J. Nat. Gas Chem. 18 (2009) 167–172 10.1016/S1003-9953(08)60098-5.

[60] S. Karka, S. Kodukula, S.V Nandury, U. Pal, Polyethylenimine-modified zeolite 13X for CO_2 capture: adsorption and kinetic studies, ACS Omega 4 (2019) 16441–16449 10.1021/acsomega.9b02047.

[61] K. Li, J. Jiang, F. Yan, S. Tian, X. Chen, The influence of polyethyleneimine type and molecular weight on the CO_2 capture performance of PEI-nano silica adsorbents, Appl. Energy. 136 (2014) 750–755 10.1016/j.apenergy.2014.09.057.

[62] C. Perinu, G. Saramakoon, B. Arstad, K.-J. Jens, Application of 15N-NMR spectroscopy to analysis of amine based CO_2 capture solvents, Energy Procedia 63 (2014) 1144–1150 10.1016/j.egypro.2014.11.124.

[63] P. Singh, J.P.M. Niederer, G.F. Versteeg, Structure and activity relationships for amine-based CO_2 absorbents-II, Chem. Eng. Res. Des. 87 (2009) 135–144 10.1016/j.cherd.2008.07.014.

[64] P. Singh, J.P.M. Niederer, G.F. Versteeg, Structure and activity relationships for amine based CO_2 absorbents—I, Int. J. Greenh. Gas Control. 1 (2007) 5–10 10.1016/S1750-5836(07)00015-1.

[65] H. Thakkar, A. Issa, A.A. Rownaghi, F. Rezaei, CO_2 capture from air using amine-functionalized kaolin-based zeolites, Chem. Eng. Technol. 40 (2017) 1999–2007 10.1002/ceat.201700188.

[66] M. Davidson, Y. Ji, G.J. Leong, N.C. Kovach, B.G. Trewyn, R.M. Richards, Hybrid mesoporous silica/noble-metal nanoparticle materials—synthesis and catalytic applications, ACS Appl. Nano Mater. 1 (2018) 4386–4400 10.1021/acsanm.8b00967.

[67] S. Nasreen, A. Urooj, U. Rafique, S. Ehrman, Functionalized mesoporous silica: absorbents for water purification, Desalin. Water Treat. 57 (2016) 29352–29362 10.1080/19443994.2016.1185744.

[68] G.K. Nasrallah, Y. Zhang, M.M. Zagho, H.M. Ismail, A.A. Al khalaf, R.M. Prieto, K.E. Albinali, A.A. Elzatahry, Y. Deng, A systematic investigation of the bio-toxicity of core-shell magnetic mesoporous silica microspheres using zebrafish model, Microporous Mesoporous Mater. (2018) 10.1016/j.micromeso.2018.02.008.

[69] Y. Zhang, Q. Yue, M.M. Zagho, J. Zhang, A.A. Elzatahry, Y. Jiang, Y. Deng, Core–shell magnetic mesoporous silica microspheres with large mesopores for enzyme immobilization in biocatalysis, ACS Appl. Mater. Interfaces. 11 (2019) 10356–10363 10.1021/acsami.8b18721.

[70] X. Liang, M. Yu, J. Li, Y.-B. Jiang, A.W. Weimer, Ultra-thin microporous–mesoporous metal oxide films prepared by molecular layer deposition (MLD), Chem. Commun. (2009) 7140–7142 10.1039/B911888H.

[71] S. Zheng, H.R. Heydenrych, A. Jentys, J.A. Lercher, Influence of surface modification on the acid site distribution of HZSM-5, J. Phys. Chem. B. 106 (2002) 9552–9558 10.1021/jp014091d.

[72] Y.-H. Yue, Y. Tang, Y. Liu, Z. Gao, Chemical liquid deposition zeolites with controlled pore-opening size and shape-selective separation of isomers, Ind. Eng. Chem. Res. 35 (1996) 430–433 10.1021/ie9502648.

[73] Y. Wang, R.T. Yang, Chemical liquid deposition modified 4A zeolite as a size-selective adsorbent for methane upgrading, CO_2 capture and air separation, ACS Sustain. Chem. Eng. 7 (2019) 3301–3308 10.1021/acssuschemeng.8b05339.

[74] S.S. Kaye, A. Dailly, O.M. Yaghi, J.R. Long, Impact of preparation and handling on the hydrogen storage properties of Zn_4O(1,4-benzenedicarboxylate)3 (MOF-5), J. Am. Chem. Soc. 129 (2007) 14176–14177 10.1021/ja076877g.

[75] P. Nugent, Y. Belmabkhout, S.D. Burd, A.J. Cairns, R. Luebke, K. Forrest, T. Pham, S. Ma, B. Space, L. Wojtas, M. Eddaoudi, M.J. Zaworotko, Porous materials with optimal adsorption thermodynamics and kinetics for CO_2 separation, Nature 495 (2013) 80–84 10.1038/nature11893.

[76] F. Gao, Y. Li, Z. Bian, J. Hu, H. Liu, Dynamic hydrophobic hindrance effect of zeolite@zeolitic imidazolate framework composites for CO_2 capture in the presence of water, J. Mater. Chem. A. 3 (2015) 8091–8097 10.1039/C4TA06645F.

[77] K.-M. Lee, Y.-H. Lim, C.-J. Park, Y.-M. Jo, Adsorption of Low-Level CO_2 using modified zeolites and activated carbon, Ind. Eng. Chem. Res. 51 (2012) 1355–1363 10.1021/ie2013532.

[78] E.P. Reddy, P.G. Smirniotis, High-temperature sorbents for CO_2 made of alkali metals doped on CaO supports, J. Phys. Chem. B. 108 (2004) 7794–7800 10.1021/jp031245b.

[79] E. Díaz, E. Muñoz, A. Vega, S. Ordóñez, Enhancement of the CO2 retention capacity of X zeolites by Na- and Cs-treatments, Chemosphere 70 (2008) 1375–1382 10.1016/j.chemosphere.2007.09.034.

[80] M. Sun, Q. Gu, A. Hanif, T. Wang, J. Shang, Transition metal cation-exchanged SSZ-13 zeolites for CO_2 capture and separation from N_2, Chem. Eng. J. 370 (2019) 1450–1458 http://www.sciencedirect.com/science/article/pii/S1385894719307089.

[81] Q. Jiang, J. Rentschler, G. Sethia, S. Weinman, R. Perrone, K. Liu, Synthesis of T-type zeolite nanoparticles for the separation of CO_2/N_2 and CO_2/CH_4 by adsorption process, Chem. Eng. J. 230 (2013) 380–388 10.1016/j.cej.2013.06.103.

[82] G. Singh, S. Tiburcius, S.M. Ruban, D. Shanbhag, C.I. Sathish, K. Ramadass, A. Vinu, Pure and strontium carbonate nanoparticles functionalized microporous carbons with high specific surface areas derived from chitosan for CO_2 adsorption, Emergent Mater. 2 (2019) 337–349 10.1007/s42247-019-00050-8.

[83] D. Shakarova, A. Ojuva, L. Bergström, F. Akhtar, Methylcellulose-directed synthesis of nanocrystalline zeolite NaA with high CO_2 uptake, Materials (Basel) 7 (2014) 5507–5519 10.3390/ma7085507.

[84] H. Zhou, Y. Li, G. Zhu, J. Liu, W. Yang, Microwave-assisted hydrothermal synthesis of a&b-oriented zeolite T membranes and their pervaporation properties, Sep. Purif. Technol. 65 (2009) 164–172 10.1016/j.seppur.2008.10.046.

[85] K.P. Lillerud, J.H. Raeder, On the synthesis of erionite—offretite intergrowth zeolites, Zeolites 6 (1986) 474–483 10.1016/0144-2449(86)90032-1.

[86] V.P. Valtchev, L. Tosheva, K.N. Bozhilov, Synthesis of zeolite nanocrystals at room temperature, Langmuir 21 (2005) 10724–10729 10.1021/la050323e.

[87] L. Tosheva, V.P. Valtchev, Nanozeolites: synthesis, crystallization mechanism, and applications, Chem. Mater. 17 (2005) 2494–2513 10.1021/cm047908z.

[88] X. Liu, Y. Wang, X. Cui, Y. He, J. Mao, Influence of synthesis parameters on NaA zeolite crystals, Powder Technol. 243 (2013) 184–193 10.1016/j.powtec.2013.03.048.

[89] X. Zhang, D. Tang, G. Jiang, Synthesis of zeolite NaA at room temperature: the effect of synthesis parameters on crystal size and its size distribution, Adv. Powder Technol. 24 (2013) 689–696 10.1016/j.apt.2012.12.010.

[90] M. Moliner, Direct synthesis of functional zeolitic materials, ISRN Mater. Sci. 2012 (2012) 789525 10.5402/2012/789525.

[91] O. Cheung, Z. Bacsik, Q. Liu, A. Mace, N. Hedin, Adsorption kinetics for CO_2 on highly selective zeolites NaKA and nano-NaKA, Appl. Energy. 112 (2013) 1326–1336 http://www.sciencedirect.com/science/article/pii/S0306261913000263.

[92] H. Fong, I. Chun, D.H. Reneker, Beaded nanofibers formed during electrospinning, Polymer (Guildf) 40 (1999) 4585–4592 10.1016/S0032-3861(99)00068-3.

[93] J.M. Deitzel, W. Kosik, S.H. McKnight, N.C. Beck Tan, J.M. DeSimone, S. Crette, Electrospinning of polymer nanofibers with specific surface chemistry, Polymer (Guildf) 43 (2002) 1025–1029 10.1016/S0032-3861(01)00594-8.

[94] Y.M. Shin, M.M. Hohman, M.P. Brenner, G.C. Rutledge, Experimental characterization of electrospinning : the electrically forced jet and instabilities, Polymer (Guildf) 42 (2001) 9955–9967.

[95] A. Calderon, M.C. Que, A. Premacio, D. Marasigan, Morphological characterization of electrospun zeolite-filled Acrylonitrile Butadiene Styrene fibrous membrane for low-pressured CO_2 adsorption, Sustain. Environ. Res. 24 (2014) 365–371.

[96] J. Liu, G. Jiang, Y. Liu, J. Di, Y. Wang, Z. Zhao, Q. Sun, C. Xu, J. Gao, A. Duan, J. Liu, Y. Wei, Y. Zhao, L. Jiang, Hierarchical macro-meso-microporous ZSM-5 zeolite hollow fibers with highly efficient catalytic cracking capability, Sci. Rep. 4 (2014) 7276 10.1038/srep07276.

[97] S.H. Ji, J.H. Cho, Y.H. Jeong, J. Do Yun, J.S. Yun, The synthesis of flexible zeolite nanofibers by a polymer surface thermal etching process, Appl. Surf. Sci. 416 (2017) 178–182 http://www.sciencedirect.com/science/article/pii/S0169433217310930.

[98] W. Zhang, K. Narang, S.B. Simonsen, N.M. Vinkel, M. Gudik-Sørensen, L. Han, F. Akhtar, A. Kaiser, Highly structured nanofiber zeolite materials for biogas upgrading, Energy Technol. 8 (2020) 1900781 10.1002/ente.201900781.

[99] L. Valencia, W. Rosas, A. Aguilar-Sanchez, A.P. Mathew, A.E.C. Palmqvist, Bio-based Micro-/Meso-/Macroporous hybrid foams with ultrahigh zeolite loadings for selective capture of carbon dioxide, ACS Appl. Mater. Interfaces. 11 (2019) 40424–40431 10.1021/acsami.9b11399.

[100] M. Mazaj, M. Bjelica, E. Žagar, N.Z. Logar, S. Kovačič, Zeolite nanocrystals embedded in microcellular carbon foam as a high-performance CO_2 capture adsorbent with energy-saving regeneration properties, ChemSusChem n/a (2020) 10.1002/cssc.201903116.

[101] W.A.W.A. Bakar, R. Ali, Natural Gas, in: P. Potocnik (Ed.), Natural Gas, IntechOpen, London, UK, 2010 10.5772/9804.

[102] D.F. Mohshim, H. Mukhtar, Z. Man, A study on carbon dioxide removal by blending the ionic liquid in membrane synthesis, Sep. Purif. Technol. 196 (2018) 20–26 10.1016/j.seppur.2017.06.034.

[103] N. Jusoh, Y.F. Yeong, T.L. Chew, K.K. Lau, A.M. Shariff, Current development and challenges of mixed matrix membranes for CO_2/CH_4 separation, Sep. Purif. Rev. 45 (2016) 321–344 10.1080/15422119.2016.1146149.

[104] S. Shah, M. Shah, A. Shah, M. Shah, Evolution in the membrane-based materials and comprehensive review on carbon capture and storage in industries, Emergent Mater. 3 (2020) 33–44 10.1007/s42247-020-00069-2.

[105] Z. Dai, L. Ansaloni, L. Deng, Recent advances in multi-layer composite polymeric membranes for CO_2 separation: a review, Green Energy Environ. 1 (2016) 102–128 http://www.sciencedirect.com/science/article/pii/S2468025716300279.

[106] H. Verweij, Inorganic membranes, Curr. Opin. Chem. Eng. 1 (2012) 156–162 http://www.sciencedirect.com/science/article/pii/S2211339812000172.

[107] H. Li, K. Haas-Santo, U. Schygulla, R. Dittmeyer, Inorganic microporous membranes for H_2 and CO_2 separation—review of experimental and modeling progress, Chem. Eng. Sci. 127 (2015) 401–417 http://www.sciencedirect.com/science/article/pii/S0009250915000421.

[108] T.-S. Chung, L.Y. Jiang, Y. Li, S. Kulprathipanja, Mixed matrix membranes (MMMs) comprising organic polymers with dispersed inorganic fillers for gas separation, Prog. Polym. Sci. 32 (2007) 483–507 http://www.sciencedirect.com/science/article/pii/S0079670007000081.

[109] Y. Jiang, C. Liu, J. Caro, A. Huang, A new UiO-66-NH2 based mixed-matrix membranes with high CO_2/CH_4 separation performance, Microporous Mesoporous Mater 274 (2019) 203–211 http://www.sciencedirect.com/science/article/pii/S138718111830430X.

[110] H. Cong, M. Radosz, B.F. Towler, Y. Shen, Polymer–inorganic nanocomposite membranes for gas separation, Sep. Purif. Technol. 55 (2007) 281–291 http://www.sciencedirect.com/science/article/pii/S1383586606004369.

[111] P.S. Goh, A.F. Ismail, S.M. Sanip, B.C. Ng, M. Aziz, Recent advances of inorganic fillers in mixed matrix membrane for gas separation, Sep. Purif. Technol. 81 (2011) 243–264 http://www.sciencedirect.com/science/article/pii/S1383586611004503.

[112] R. Mahajan, D.Q. Vu, W.J. Koros, Mixed matrix membrane materials: an answer to the challenges faced by membrane based gas separations today? J. Chin. Inst. Chem. Eng. 33 (2002) 77–86.

[113] S. Saqib, S. Rafiq, M. Chawla, M. Saeed, N. Muhammad, S. Khurram, K. Majeed, A.L. Khan, M. Ghauri, F. Jamil, M. Aslam, Facile CO2 Separation in Composite Membranes, Chem. Eng. Technol. 42 (2019) 30–44 10.1002/ceat.201700653.

[114] R. Surya Murali, A.F. Ismail, M.A. Rahman, S. Sridhar, Mixed matrix membranes of Pebax-1657 loaded with 4A zeolite for gaseous separations, Sep. Purif. Technol. 129 (2014) 1–8 10.1016/j.seppur.2014.03.017.

[115] S. Meshkat, S. Kaliaguine, D. Rodrigue, Mixed matrix membranes based on amine and non-amine MIL-53(Al) in Pebax® MH-1657 for CO_2 separation, Sep. Purif. Technol. 200 (2018) 177–190 10.1016/j.seppur.2018.02.038.

[116] J.E. Shin, S.K. Lee, Y.H. Cho, H.B. Park, Effect of PEG-MEA and graphene oxide additives on the performance of Pebax®1657 mixed matrix membranes for CO_2 separation, J. Memb. Sci. 572 (2019) 300–308 10.1016/j.memsci.2018.11.025.

[117] R. Castro-Muñoz, V. Fíla, Progress on incorporating zeolites in matrimid® 5218 mixed matrix membranes towards gas separation, Membranes (Basel) 8 (2018) 1–23 10.3390/membranes8020030.

[118] D. Carter, F.H. Tezel, B. Kruczek, H. Kalipcilar, Investigation and comparison of mixed matrix membranes composed of polyimide matrimid with ZIF – 8, silicalite, and SAPO – 34, J. Memb. Sci. 544 (2017) 35–46 10.1016/j.memsci.2017.08.068.

[119] E.M. Mahdi, J.-C. Tan, Mixed-matrix membranes of zeolitic imidazolate framework (ZIF-8)/Matrimid nanocomposite: thermo-mechanical stability and viscoelasticity underpinning membrane separation performance, J. Memb. Sci. 498 (2016) 276–290 10.1016/j.memsci.2015.09.066.

[120] J. Ahmad, M.-B. Hägg, Development of matrimid/zeolite 4A mixed matrix membranes using low boiling point solvent, Sep. Purif. Technol. 115 (2013) 190–197 10.1016/j.seppur.2013.04.049.

[121] M.B. Mohamad, Y.Y. Fong, A. Shariff, Gas separation of carbon dioxide from methane using polysulfone membrane incorporated with zeolite-T, Procedia Eng 148 (2016) 621–629 10.1016/j.proeng.2016.06.526.

[122] M. Sarfraz, M. Ba-Shammakh, Synergistic effect of adding graphene oxide and ZIF-301 to polysulfone to develop high performance mixed matrix membranes for selective carbon dioxide separation from post combustion flue gas, J. Memb. Sci. 514 (2016) 35–43 10.1016/j.memsci.2016.04.029.

[123] S. Shahid, K. Nijmeijer, Matrimid®/polysulfone blend mixed matrix membranes containing ZIF-8 nanoparticles for high pressure stability in natural gas separation, Sep. Purif. Technol. 189 (2017) 90–100 10.1016/j.seppur.2017.07.075.

[124] M. Safak Boroglu, A.B. Yumru, Gas separation performance of 6FDA-DAM-ZIF-11 mixed-matrix membranes for H_2/CH_4 and CO_2/CH_4 separation, Sep. Purif. Technol. 173 (2017) 269–279 10.1016/j.seppur.2016.09.037.

[125] M. Etxeberria-Benavides, O. David, T. Johnson, M.M. Łozińska, A. Orsi, P.A. Wright, S. Mastel, R. Hillenbrand, F. Kapteijn, J. Gascon, High performance

mixed matrix membranes (MMMs) composed of ZIF-94 filler and 6FDA-DAM polymer, J. Memb. Sci. 550 (2018) 198–207 10.1016/j.memsci.2017.12.033.
[126] M.Z. Ahmad, M. Navarro, M. Lhotka, B. Zornoza, C. Téllez, W.M. de Vos, N.E. Benes, N.M. Konnertz, T. Visser, R. Semino, G. Maurin, V. Fila, J. Coronas, Enhanced gas separation performance of 6FDA-DAM based mixed matrix membranes by incorporating MOF UiO-66 and its derivatives, J. Memb. Sci. 558 (2018) 64–77 10.1016/j.memsci.2018.04.040.
[127] O.G. Nik, X.Y. Chen, S. Kaliaguine, Amine-functionalized zeolite FAU/EMT-polyimide mixed matrix membranes for CO_2/CH_4 separation, J. Memb. Sci. 379 (2011) 468–478 10.1016/j.memsci.2011.06.019.
[128] A. Ebadi Amooghin, M. Omidkhah, A. Kargari, The effects of aminosilane grafting on NaY zeolite–Matrimid®5218 mixed matrix membranes for CO_2/CH_4 separation, J. Memb. Sci. 490 (2015) 364–379 10.1016/j.memsci.2015.04.070.
[129] N. Jusoh, Y.F. Yeong, K.K. Lau, A.M. Shariff, Fabrication of silanated zeolite T/6FDA-durene composite membranes for CO_2/CH_4 separation, J. Clean. Prod. 166 (2017) 1043–1058 10.1016/j.jclepro.2017.08.080.
[130] D. Eiras, Y. Labreche, L.A. Pessan, UltemÂ®/ZIF-8 mixed matrix membranes for gas separation: transport and physical properties, Mater. Res. 19 (2016) 220–228 http://www.scielo.br/scielo.php?script=sci_arttext&pid=S1516-14392016000100220&nrm=iso.
[131] Ó. de la Iglesia, S. Sorribas, E. Almendro, B. Zornoza, C. Téllez, J. Coronas, Metal-organic framework MIL-101(Cr) based mixed matrix membranes for esterification of ethanol and acetic acid in a membrane reactor, Renew. Energy. 88 (2016) 12–19 10.1016/j.renene.2015.11.025.
[132] M. Waqas Anjum, B. Bueken, D. De Vos, I.F.J. Vankelecom, MIL-125(Ti) based mixed matrix membranes for CO_2 separation from CH_4 and N_2, J. Memb. Sci. 502 (2016) 21–28 10.1016/j.memsci.2015.12.022.
[133] A.F. Ismail, P.S. Goh, S.M. Sanip, M. Aziz, Transport and separation properties of carbon nanotube-mixed matrix membrane, Sep. Purif. Technol. 70 (2009) 12–26 10.1016/j.seppur.2009.09.002.
[134] M. Waqas Anjum, F. de Clippel, J. Didden, A. Laeeq Khan, S. Couck, G.V Baron, J.F.M. Denayer, B.F. Sels, I.F.J. Vankelecom, Polyimide mixed matrix membranes for CO_2 separations using carbon–silica nanocomposite fillers, J. Memb. Sci. 495 (2015) 121–129 10.1016/j.memsci.2015.08.006.
[135] D.Q. Vu, W.J. Koros, S.J. Miller, Mixed matrix membranes using carbon molecular sieves: II. Modeling permeation behavior, J. Memb. Sci. 211 (2003) 335–348 10.1016/S0376-7388(02)00425-8.
[136] B. Zornoza, B. Seoane, J.M. Zamaro, C. Téllez, J. Coronas, Combination of MOFs and zeolites for mixed-matrix membranes, ChemPhysChem 12 (2011) 2781–2785 10.1002/cphc.201100583.
[137] S. Rafiq, Z. Man, S. Maitra, N. Muhammad, F. Ahmad, Kinetics of thermal degradation of polysulfone/polyimide blended polymeric membranes, J. Appl. Polym. Sci. 123 (2012) 3755–3763 10.1002/app.34862.
[138] S. Alexander Stern, Polymers for gas separations: the next decade, J. Memb. Sci. 94 (1994) 1–65 10.1016/0376-7388(94)00141-3.
[139] J.G. Wijmans, R.W. Baker, The solution-diffusion model: a review, J. Memb. Sci. 107 (1995) 1–21 10.1016/0376-7388(95)00102-I.
[140] N. Widjojo, Y. Li, L.Y. Jiang, T.-S. Chung, Recent progress and challenges on mixed matrix membranes in both material and configuration aspects for gas separation, in: M.G. Buonomenna, G. Golemme (Eds.), Adv. Mater. Membr. Prep., 1st ed., Bentham Science, 2012, pp. 64–82. 10.2174/97816080530871120101.
[141] O. Bakhtiari, N. Sadeghi, The formed voids around the filler particles impact on the mixed matrix membranes' gas permeabilities, Int. J. Chem. Eng. Appl. 5 (2014) 198–203 10.7763/ijcea.2014.v5.378.
[142] R.D. Noble, Perspectives on mixed matrix membranes, J. Memb. Sci. 378 (2011) 393–397 10.1016/j.memsci.2011.05.031.
[143] M. Rezakazemi, A. Ebadi Amooghin, M.M. Montazer-Rahmati, A.F. Ismail, T. Matsuura, State-of-the-art membrane based CO_2 separation using mixed matrix membranes (MMMs): an overview on current status and future directions, Prog. Polym. Sci. 39 (2014) 817–861 10.1016/j.progpolymsci.2014.01.003.
[144] R. Lin, B. Villacorta Hernandez, L. Ge, Z. Zhu, Metal organic framework based mixed matrix membranes: an overview on filler/polymer interfaces, J. Mater. Chem. A. 6 (2018) 293–312 10.1039/C7TA07294E.
[145] V.C. Souza, M.G.N. Quadri, Organic-inorganic hybrid membranes in separation processes: a 10-year review, Brazilian J. Chem. Eng. 30 (2013) 683–700 http://www.scielo.br/scielo.php?script=sci_arttext&pid=S0104-66322013000400001&nrm=iso.
[146] R. Lin, L. Ge, L. Hou, E. Strounina, V. Rudolph, Z. Zhu, Mixed matrix membranes with strengthened MOFs/polymer interfacial interaction and improved membrane performance, ACS Appl. Mater. Interfaces. 6 (2014) 5609–5618 10.1021/am500081e.
[147] T. Yang, Y. Xiao, T.-S. Chung, Poly-/metal-benzimidazole nano-composite membranes for hydrogen purification, Energy Environ. Sci. 4 (2011) 4171–4180 10.1039/C1EE01324F.
[148] T.-H. Bae, J.S. Lee, W. Qiu, W.J. Koros, C.W. Jones, S. Nair, A high-performance gas-separation membrane containing submicrometer-sized metal–organic framework crystals, Angew. Chemie Int. Ed. 49 (2010) 9863–9866 10.1002/anie.201006141.
[149] Y. Li, H.-M. Guan, T.-S. Chung, S. Kulprathipanja, Effects of novel silane modification of zeolite surface on polymer chain rigidification and partial pore blockage in polyethersulfone (PES)–zeolite A mixed matrix membranes, J. Memb. Sci. 275 (2006) 17–28 10.1016/j.memsci.2005.08.015.
[150] Y. Li, T.-S. Chung, C. Cao, S. Kulprathipanja, The effects of polymer chain rigidification, zeolite pore size and pore blockage on polyethersulfone (PES)-zeolite A mixed matrix membranes, J. Memb. Sci. 260 (2005) 45–55 10.1016/j.memsci.2005.03.019.
[151] G. Clarizia, C. Algieri, E. Drioli, Filler-polymer combination: a route to modify gas transport properties of a polymeric membrane, Polymer (Guildf) 45 (2004) 5671–5681 10.1016/j.polymer.2004.06.001.
[152] T.C. Merkel, B.D. Freeman, R.J. Spontak, Z. He, I. Pinnau, P. Meakin, A.J. Hill, Sorption, transport, and structural evidence for enhanced free volume in poly(4-methyl-2-pentyne)/fumed silica nanocomposite membranes, Chem. Mater. 15 (2003) 109–123 10.1021/cm020672j.
[153] M. Moaddeb, W.J. Koros, Gas transport properties of thin polymeric membranes in the presence of silicon dioxide particles, J. Memb. Sci. 125 (1997) 143–163 10.1016/S0376-7388(96)00251-7.
[154] B. Zornoza, S. Irusta, C. Téllez, J. Coronas, Mesoporous silica sphere−polysulfone mixed matrix membranes for gas separation, Langmuir 25 (2009) 5903–5909 10.1021/la900656z.
[155] B. Zornoza, C. Téllez, J. Coronas, Mixed matrix membranes comprising glassy polymers and dispersed mesoporous silica spheres for gas separation, J. Memb. Sci. 368 (2011) 100–109 10.1016/j.memsci.2010.11.027.
[156] B. Zornoza, C. Téllez, J. Coronas, O. Esekhile, W.J. Koros, Mixed matrix membranes based on 6FDA polyimide with silica and zeolite microsphere dispersed phases, AIChE J. 61 (2015) 4481–4490 10.1002/aic.15011.
[157] L. Ge, W. Zhou, V. Rudolph, Z. Zhu, Mixed matrix membranes incorporated with size-reduced Cu-BTC for improved gas separation, J. Mater. Chem. A. 1 (2013) 6350–6358 10.1039/C3TA11131H.
[158] B. Seoane, V. Sebastián, C. Téllez, J. Coronas, Crystallization in THF: the possibility of one-pot synthesis of mixed matrix membranes containing MOF MIL-68(Al), CrystEngComm 15 (2013) 9483–9490 10.1039/C3CE40847G.
[159] L. Diestel, N. Wang, B. Schwiedland, F. Steinbach, U. Giese, J. Caro, MOF based MMMs with enhanced selectivity due to hindered linker distortion, J. Memb. Sci. 492 (2015) 181–186 10.1016/j.memsci.2015.04.069.
[160] A. Sabetghadam, B. Seoane, D. Keskin, N. Duim, T. Rodenas, S. Shahid, S. Sorribas, C.Le Guillouzer, G. Clet, C. Tellez, M. Daturi, J. Coronas, F. Kapteijn, J. Gascon, Metal organic framework crystals in mixed-matrix membranes: impact of the filler morphology on the gas separation performance, Adv. Funct. Mater. 26 (2016) 3154–3163 10.1002/adfm.201505352.
[161] N. Tien-Binh, D. Rodrigue, S. Kaliaguine, In-situ cross interface linking of PIM-1 polymer and UiO-66-NH_2 for outstanding gas separation and physical aging control, J. Memb. Sci. 548 (2018) 429–438 10.1016/j.memsci.2017.11.054.
[162] J.-M. Duval, A.J.B. Kemperman, B. Folkers, M.H.V Mulder, G. Desgrandchamps, C.A. Smolders, Preparation of zeolite filled glassy polymer membranes, J. Appl. Polym. Sci. 54 (1994) 409–418 10.1002/app.1994.070540401.
[163] H.H. Yong, H.C. Park, Y.S. Kang, J. Won, W.N. Kim, Zeolite-filled polyimide membrane containing 2,4,6-triaminopyrimidine, J. Memb. Sci. 188 (2001) 151–163 10.1016/S0376-7388(00)00659-1.
[164] R. Mahajan, W.J. Koros, Mixed matrix membrane materials with glassy polymers. Part 2, Polym. Eng. Sci. 7 (2002) 1432–1441 10.1002/pen.11042.
[165] E.E. Oral, Effect of operating parameters on perforamnce of additive/zeolite/polymer mixed matrix membranes PhD thesis, Middle East Technical University, Ankara, Turkey, 2011.
[166] O. Bakhtiari, S. Mosleh, T. Khosravi, T. Mohammadi, Preparation, characterization and gas permeation of polyimide mixed matrix membranes, J. Membr. Sci. Technol. 01 (2011) 1–8 10.4172/2155-9589.1000101.
[167] W.J. Koros, D.Q. Vu, R. Mahajan, S.J. Miller, Gas separations using mixed matrix membranes. U.S. Patent US 6503295 B1, 2003.
[168] A.M.W. Hillock, S.J. Miller, W.J. Koros, Crosslinked mixed matrix membranes for the purification of natural gas: effects of sieve surface modification, J. Memb. Sci. 314 (2008) 193–199 10.1016/j.memsci.2008.01.046.
[169] D.Q. Vu, W.J. Koros, S.J. Miller, Mixed matrix membranes using carbon molecular sieves: I. Preparation and experimental results, J. Memb. Sci. 211 (2003) 311–334 10.1016/S0376-7388(02)00429-5.
[170] X. Guo, Z. Qiao, D. Liu, C. Zhong, Mixed-matrix membranes for CO_2 separation: role of the third component, J. Mater. Chem. A. 7 (2019) 24738–24759 10.1039/C9TA09012F.
[171] M.U.M. Junaidi, C.P. Khoo, C.P. Leo, A.L. Ahmad, The effects of solvents on the modification of SAPO-34 zeolite using 3-aminopropyl trimethoxy silane for the preparation of asymmetric polysulfone mixed matrix membrane in the application of CO_2 separation, Microporous Mesoporous Mater. 192 (2014) 52–59 10.1016/j.micromeso.2013.10.006.
[172] S. Husain, Mixed Matrix Dual Layer Hollow Fiber Membranes for Natural Gas Separation, Georgia Institute of Technology, Atlanta, Georgia, 2006 PhD thesis https://smartech.gatech.edu/handle/1853/16178 .
[173] K. Miyatake, O. Ohama, Y. Kawahara, A. Urano, A. Kimura, Study on analysis method for reaction of silane coupling agent on inorganic materials, SEI Tech. Rev. 65 (2007) 21–24.
[174] J. Faucheu, C. Gauthier, L. Chazeau, J.-Y. Cavaillé, V. Mellon, E.B. Lami, Miniemulsion polymerization for synthesis of structured clay/polymer nanocomposites: short review and recent advances, Polymer (Guildf) 51 (2010) 6–17 10.1016/j.polymer.2009.11.044.
[175] L. Shao, C.-H. Lau, T.-S. Chung, A novel strategy for surface modification of polyimide membranes by vapor-phase ethylenediamine (EDA) for hydrogen purification, Int. J. Hydrog. Energy. 34 (2009) 8716–8722 10.1016/j.ijhydene.2009.07.115.
[176] L. Shao, T.-S. Chung, In situ fabrication of cross-linked PEO/silica reverse-selective membranes for hydrogen purification, Int. J. Hydrog. Energy. 34 (2009) 6492–6504 10.1016/j.ijhydene.2009.05.137.
[177] H. Sanaeepur, A.E. Amooghin, A. Moghadassi, A. Kargari, Preparation and characterization of acrylonitrile–butadiene–styrene/poly(vinyl acetate)

membrane for CO_2 removal, Sep. Purif. Technol. 80 (2011) 499–508 10.1016/j.seppur.2011.06.003.
[178] A. Ebadi Amooghin, H. Sanaeepur, A. Kargari, A. Moghadassi, Direct determination of concentration-dependent diffusion coefficient in polymeric membranes based on the Frisch method, Sep. Purif. Technol. 82 (2011) 102–113 10.1016/j.seppur.2011.08.031.
[179] M. Sadrzadeh, K. Shahidi, T. Mohammadi, Preparation and C_3H_8/gas separation properties of a synthesized single layer PDMS membrane, Sep. Sci. Technol. 45 (2010) 592–603 10.1080/01496390903562530.
[180] A. Ghadimi, M. Sadrzadeh, T. Mohammadi, Prediction of ternary gas permeation through synthesized PDMS membranes by using Principal Component Analysis (PCA) and fuzzy logic (FL), J. Memb. Sci. 360 (2010) 509–521 10.1016/j.memsci.2010.05.055.
[181] P. Moradi Shehni, A.E. Amooghin, A. Ghadimi, M. Sadrzadeh, T. Mohammadi, Modeling of unsteady-state permeation of gas mixture through a self-synthesized PDMS membranes, Sep. Purif. Technol. 76 (2011) 385–399 10.1016/j.seppur.2010.11.010.
[182] M. Sadrzadeh, M. Amirilargani, K. Shahidi, T. Mohammadi, Pure and mixed gas permeation through a composite polydimethylsiloxane membrane, Polym. Adv. Technol. 22 (2011) 586–597 10.1002/pat.1551.
[183] G. Lin, M. Abar, L.M. Vane, Mixed matrix silicone and fluorosilicone/zeolite 4A membranes for ethanol dehydration by pervaporation, Sep. Sci. Technol. 48 (2013) 523–536 10.1080/01496395.2012.719057.
[184] Ş.B. Tantekin-Ersolmaz, Ç. Atalay-Oral, M. Tatlıer, A. Erdem-Şenatalar, B. Schoeman, J. Sterte, Effect of zeolite particle size on the performance of polymer–zeolite mixed matrix membranes, J. Memb. Sci. 175 (2000) 285–288 10.1016/S0376-7388(00)00423-3.
[185] M. Hussain, A. König, Mixed-matrix membrane for gas separation: polydimethylsiloxane filled with zeolite, Chem. Eng. Technol. 35 (2012) 561–569 10.1002/ceat.201100419.
[186] M. Rezakazemi, K. Shahidi, T. Mohammadi, Hydrogen separation and purification using crosslinkable PDMS/zeolite A nanoparticles mixed matrix membranes, Int. J. Hydrogen Energy. 37 (2012) 14576–14589 10.1016/j.ijhydene.2012.06.104.
[187] J.-M. Duval, B. Folkers, M.H.V Mulder, G. Desgrandchamps, C.A. Smolders, Adsorbent filled membranes for gas separation. Part 1. Improvement of the gas separation properties of polymeric membranes by incorporation of microporous adsorbents, J. Memb. Sci. 80 (1993) 189–198 10.1016/0376-7388(93)85143-K.
[188] R.T. Adams, J.S. Lee, T.-H. Bae, J.K. Ward, J.R. Johnson, C.W. Jones, S. Nair, W.J. Koros, CO_2–CH_4 permeation in high zeolite 4A loading mixed matrix membranes, J. Memb. Sci. 367 (2011) 197–203 10.1016/j.memsci.2010.10.059.
[189] Z. Tahir, A. Ilyas, X. Li, M.R. Bilad, I.F.J. Vankelecom, A.L. Khan, Tuning the gas separation performance of fluorinated and sulfonated PEEK membranes by incorporation of zeolite 4A, J. Appl. Polym. Sci. 135 (2018) 45952 10.1002/app.45952.
[190] H.T. Afarani, M. Sadeghi, A. Moheb, The gas separation performance of polyurethane–zeolite mixed matrix membranes, Adv. Polym. Technol. 37 (2018) 339–348 10.1002/adv.21672.
[191] R. Mahajan, W.J. Koros, Mixed matrix membrane materials with glassy polymers. Part 1, Polym. Eng. Sci. 42 (2002) 1420–1431 10.1002/pen.11041.
[192] R. Mahajan, R. Burns, M. Schaeffer, W.J. Koros, Challenges in forming successful mixed matrix membranes with rigid polymeric materials, J. Appl. Polym. Sci. 86 (2002) 881–890 10.1002/app.10998.
[193] A. Fernández-Barquín, C. Casado-Coterillo, M. Etxeberria-Benavides, J. Zuñiga, A. Irabien, Comparison of flat and hollow-fiber mixed-matrix composite membranes for CO_2 separation with temperature, Chem. Eng. Technol. 40 (2017) 997–1007 10.1002/ceat.201600580.
[194] N.H. Suhaimi, Y.F. Yeong, C.W.M. Ch'ng, N. Jusoh, Tailoring CO_2/CH_4 separation performance of mixed matrix membranes by using ZIF-8 particles functionalized with different amine groups, Polymers (Basel) 11 (2019) 1–19 10.3390/polym11122037.
[195] X.Y. Chen, H. Vinh-Thang, D. Rodrigue, S. Kaliaguine, Amine-functionalized MIL-53 Metal–organic framework in polyimide mixed matrix membranes for CO_2/CH_4 separation, Ind. Eng. Chem. Res. 51 (2012) 6895–6906 10.1021/ie3004336.
[196] X. Guo, H. Huang, Y. Ban, Q. Yang, Y. Xiao, Y. Li, W. Yang, C. Zhong, Mixed matrix membranes incorporated with amine-functionalized titanium-based metal-organic framework for CO_2/CH_4 separation, J. Memb. Sci. 478 (2015) 130–139 10.1016/j.memsci.2015.01.007.
[197] E.V Perez, G.J.D. Kalaw, J.P. Ferraris, K.J. Balkus, I.H. Musselman, Amine-functionalized (Al) MIL-53/VTEC™ mixed-matrix membranes for H_2/CO_2 mixture separations at high pressure and high temperature, J. Memb. Sci. 530 (2017) 201–212 10.1016/j.memsci.2017.02.003.
[198] H.R. Amedi, M. Aghajani, Aminosilane-functionalized ZIF-8/PEBA mixed matrix membrane for gas separation application, Microporous Mesoporous Mater. 247 (2017) 124–135 10.1016/j.micromeso.2017.04.001.
[199] Y. Li, T.-S. Chung, S. Kulprathipanja, Novel Ag+-zeolite/polymer mixed matrix membranes with a high CO_2/CH_4 selectivity, AIChE J. 53 (2007) 610–616 10.1002/aic.11109.
[200] A. Ebadi Amooghin, M. Omidkhah, H. Sanaeepur, A. Kargari, Preparation and characterization of Ag+ ion-exchanged zeolite-Matrimid®5218 mixed matrix membrane for CO_2/CH_4 separation, J. Energy Chem. 25 (2016) 450–462 10.1016/j.jechem.2016.02.004.
[201] A. Ebadi Amooghin, H. Sanaeepur, M. Omidkhah, A. Kargari, Ship-in-a-bottle", a new synthesis strategy for preparing novel hybrid host–guest nanocomposites for highly selective membrane gas separation, J. Mater. Chem. A. 6 (2018) 1751–1771 10.1039/C7TA08081F.
[202] A. de J. Montes Luna, G. Castruita de León, S.P. García Rodríguez, N.C. Fuentes López, O. Pérez Camacho, Y.A. Perera Mercado, Na+/Ca_2+ aqueous ion exchange in natural clinoptilolite zeolite for polymer-zeolite composite membranes production and their $CH_4/CO_2/N_2$ separation performance, J. Nat. Gas Sci. Eng. 54 (2018) 47–53 10.1016/j.jngse.2018.03.007.
[203] G. Castruita-de León, C.Y. Yeverino-Miranda, A. de, J. Montes-Luna, H.I. Meléndez-Ortiz, G. Alvarado-Tenorio, L.A. García-Cerda, Amine-impregnated natural zeolite as filler in mixed matrix membranes for CO_2/CH_4 separation, J. Appl. Polym. Sci. 137 (2020) 48286 10.1002/app.48286.
[204] M.U.M. Junaidi, C.P. Leo, A.L. Ahmad, N.A. Ahmad, Fluorocarbon functionalized SAPO-34 zeolite incorporated in asymmetric mixed matrix membranes for carbon dioxide separation in wet gases, Microporous Mesoporous Mater 206 (2015) 23–33 10.1016/j.micromeso.2014.12.013.
[205] N.N.R. Ahmad, C.P. Leo, A.W. Mohammad, A.L. Ahmad, Interfacial sealing and functionalization of polysulfone/SAPO-34 mixed matrix membrane using acetate-based ionic liquid in post-impregnation for CO_2 capture, Sep. Purif. Technol. 197 (2018) 439–448 10.1016/j.seppur.2017.12.054.
[206] M.S. Maleh, A. Raisi, CO_2-philic moderate selective layer mixed matrix membranes containing surface functionalized NaX towards highly-efficient CO_2 capture, RSC Adv 9 (2019) 15542–15553 10.1039/C9RA01654F.
[207] S.S. Park, B. Ameduri, C.-S. Ha, One-pot synthesis of alkylammonium-functionalized mesoporous silica hollow spheres in water and films at the air–water interface, Emergent Mater. 2 (2019) 45–58 10.1007/s42247-019-00028-6.
[208] M.A. Sibeko, M.L. Saladino, F. Armetta, A. Spinella, A.S. Luyt, Effect of preparation method on the properties of poly(methyl methacrylate)/mesoporous silica composites, Emergent Mater. 2 (2019) 363–370 10.1007/s42247-019-00057-1.
[209] Y. Elgawady, D. Ponnamma, S. Adham, M. Al-Maas, A. Ammar, K. Alamgir, M.A.A. Al-Maadeed, M.K. Hassan, Mesoporous silica filled smart super oleophilic fibers of triblock copolymer nanocomposites for oil absorption applications, Emergent Mater. 3 (2020) 279–290 10.1007/s42247-020-00111-3.
[210] B.D. Reid, F.A. Ruiz-Trevino, I.H. Musselman, K.J. Balkus, J.P. Ferraris, Gas permeability properties of polysulfone membranes containing the mesoporous molecular sieve MCM-41, Chem. Mater. 13 (2001) 2366–2373 10.1021/cm000931.
[211] T.-H. Weng, H.-H. Tseng, M.-Y. Wey, Fabrication and characterization of poly(phenylene oxide)/SBA-15/carbon molecule sieve multilayer mixed matrix membrane for gas separation, Int. J. Hydrog. Energy. 35 (2010) 6971–6983 10.1016/j.ijhydene.2010.04.024.
[212] K. Vanherck, A. Aerts, J. Martens, I. Vankelecom, Hollow filler based mixed matrix membranes, Chem. Commun. 46 (2010) 2492–2494 10.1039/B924086A.
[213] B. Zornoza, O. Esekhile, W.J. Koros, C. Téllez, J. Coronas, Hollow silicalite-1 sphere-polymer mixed matrix membranes for gas separation, Sep. Purif. Technol. 77 (2011) 137–145 10.1016/j.seppur.2010.11.033.
[214] G. Schulz-Ekloff, J. Rathouský, A. Zukal, Mesoporous silica with controlled porous structure and regular morphology, Int. J. Inorg. Mater. 1 (1999) 97–102 10.1016/S1463-0176(99)00015-0.
[215] N. Navascués, C. Téllez, J. Coronas, Synthesis and adsorption properties of hollow silicalite-1 spheres, Microporous Mesoporous Mater. 112 (2008) 561–572 10.1016/j.micromeso.2007.10.037.
[216] S. Sinha Ray, M. Okamoto, Polymer/layered silicate nanocomposites: a review from preparation to processing, Prog. Polym. Sci. 28 (2003) 1539–1641 10.1016/j.progpolymsci.2003.08.002.
[217] H.-K. Jeong, W. Krych, H. Ramanan, S. Nair, E. Marand, M. Tsapatsis, Fabrication of polymer/selective-flake nanocomposite membranes and their use in gas separation, Chem. Mater. 16 (2004) 3838–3845 10.1021/cm049154u.
[218] W.-G. Kim, Nanoporous layered oxide materials and membranes for gas separations PhD thesis, Georgia Institute of Technology, Atlanta, Georgia, 2013.
[219] H.-K. Jeong, S. Nair, T. Vogt, L. Dickinson, M. Tsapatsis, A highly crystalline layered silicate with three-dimensionally microporous layers, Nat. Mater. 2 (2003) 53–58 10.1038/nmat795.
[220] J.-H. Wang, Q. Wei, J.-W. Cheng, H. He, B.-F. Yang, G.-Y. Yang, $Na_2B_{1_n}O_{17}$•H_2en: a three-dimensional open-framework layered borate co-templated by inorganic cations and organic amines, Chem. Commun. (Camb). 51 (2015) 5066–5068 10.1039/c5cc00800j.
[221] M. Ahmadi, S. Janakiram, Z. Dai, L. Ansaloni, L. Deng, Performance of mixed matrix membranes containing porous two-dimensional (2D) and three-dimensional (3D) fillers for CO_2 separation: a review, Membranes (Basel) 8 (2018) 50 10.3390/membranes8030050.
[222] W. Kim, J.S. Lee, D.G. Bucknall, W.J. Koros, S. Nair, Nanoporous layered silicate AMH-3/cellulose acetate nanocomposite membranes for gas separations, J. Memb. Sci. 441 (2013) 129–136 10.1016/j.memsci.2013.03.044.
[223] S. Choi, J. Coronas, J.A. Sheffel, E. Jordan, W. Oh, S. Nair, D.F. Shantz, M. Tsapatsis, Layered silicate by proton exchange and swelling of AMH-3, Microporous Mesoporous Mater. 115 (2008) 75–84 10.1016/j.micromeso.2007.12.041.
[224] S. Choi, J. Coronas, Z. Lai, D. Yust, F. Onorato, M. Tsapatsis, Fabrication and gas separation properties of polybenzimidazole (PBI)/nanoporous silicates hybrid membranes, J. Memb. Sci. 316 (2008) 145–152 10.1016/j.memsci.2007.09.026.
[225] H.J.M. Hanley, C.D. Muzny, D.L. Ho, C.J. Glinka, E. Manias, A SANS study of organoclay dispersions, Int. J. Thermophys. 22 (2001) 1435–1448 10.1023/A:1012845104722.
[226] D.L. Ho, R.M. Briber, C.J. Glinka, Characterization of organically modified clays using scattering and microscopy techniques, Chem. Mater. 13 (2001) 1923–1931 10.1021/cm0008617.
[227] C. Shang, J.A. Rice, Interpretation of small-angle x-ray scattering data from dilute montmorillonite suspensions using a modified Guinier approximation, Phys. Rev. E. 64 (2001) 021401 10.1103/PhysRevE.64.021401.
[228] E.C.N. Tzi, O.P. Ching, Surface modification of AMH-3 for development of mixed matrix membranes, Procedia Eng 148 (2016) 86–92 10.1016/j.proeng.2016.06.443.

[229] S. Choi, J. Coronas, E. Jordan, W. Oh, S. Nair, F. Onorato, D.F. Shantz, M. Tsapatsis, Layered silicates by swelling of AMH-3 and nanocomposite membranes, Angew. Chemie Int. Ed. 47 (2008) 552–555 10.1002/anie.200703440.
[230] M. Veltri, D. Vuono, P. DeLuca, J.B. Nagy, A. Nastro, Typicaldata of a new microporous material obtained from gels with titanium and silicon, J. Therm. Anal. Calorim. 84 (2006) 247–252 10.1007/s10973-005-7207-5.
[231] J. Rocha, Z. Lin, Microporous mixed octahedral-pentahedral-tetrahedral framework silicates, Rev. Mineral. Geochem. 57 (2005) 173–201 10.2138/rmg.2005.57.6.
[232] A. Galve, D. Sieffert, E. Vispe, C. Téllez, J. Coronas, C. Staudt, Copolyimide mixed matrix membranes with oriented microporous titanosilicate JDF-L1 sheet particles, J. Memb. Sci. 370 (2011) 131–140 10.1016/j.memsci.2011.01.011.
[233] M.A. Roberts, G. Sankar, J.M. Thomas, R.H. Jones, H. Du, J. Chen, W. Pang, R. Xu, Synthesis and structure of a layered titanosilicate catalyst with five-coordinate titanium, Nature 381 (1996) 401–404 10.1038/381401a0.
[234] S. Castarlenas, P. Gorgojo, C. Casado-Coterillo, S. Masheshwari, M. Tsapatsis, C. Téllez, J. Coronas, Melt compounding of swollen titanosilicate JDF-L1 with polysulfone to obtain mixed matrix membranes for H_2/CH_4 Separation, Ind. Eng. Chem. Res. 52 (2013) 1901–1907 10.1021/ie3031136.
[235] A. Galve, D. Sieffert, C. Staudt, M. Ferrando, C. Güell, C. Téllez, J. Coronas, Combination of ordered mesoporous silica MCM-41 and layered titanosilicate JDF-L1 fillers for 6FDA-based copolyimide mixed matrix membranes, J. Memb. Sci. 431 (2013) 163–170 10.1016/j.memsci.2012.12.046.
[236] J. Pérez-Carvajal, P. Lalueza, C. Casado, C. Téllez, J. Coronas, Layered titanosilicates JDF-L1 and AM-4 for biocide applications, Appl. Clay Sci. 56 (2012) 30–35 10.1016/j.clay.2011.11.020.
[237] J. Choi, M. Tsapatsis, MCM-22/Silica selective flake nanocomposite membranes for hydrogen separations, J. Am. Chem. Soc. 132 (2010) 448–449 10.1021/ja908864g.
[238] C. Rubio, C. Casado, P. Gorgojo, F. Etayo, S. Uriel, C. Téllez, J. Coronas, Exfoliated titanosilicate material UZAR-S1 obtained from JDF-L1, Eur. J. Inorg. Chem. 2010 (2010) 159–163 10.1002/ejic.200900915.
[239] K.S. Park, Z. Ni, A.P. Côté, J.Y. Choi, R. Huang, F.J. Uribe-Romo, H.K. Chae, M. O'Keeffe, O.M. Yaghi, Exceptional chemical and thermal stability of zeolitic imidazolate frameworks, Proc. Natl. Acad. Sci. 103 (2006) 10186–10191 10.1073/pnas.0602439103.
[240] N. Azizi, M.R. Hojjati, Using Pebax-1074/ZIF-7 mixed matrix membranes for separation of CO_2 from CH_4, Pet. Sci. Technol. 36 (2018) 993–1000 10.1080/10916466.2018.1458120.
[241] J. Gao, H. Mao, H. Jin, C. Chen, A. Feldhoff, Y. Li, Functionalized ZIF-7/Pebax® 2533 mixed matrix membranes for CO_2/N_2 separation, Microporous Mesoporous Mater 297 (2020) 110030 10.1016/j.micromeso.2020.110030.
[242] M. Gholami, T. Mohammadi, S. Mosleh, M. Hemmati, CO2/CH4 separation using mixed matrix membrane-based polyurethane incorporated with ZIF-8 nanoparticles, Chem. Pap. 71 (2017) 1839–1853 10.1007/s11696-017-0177-9.
[243] J.S. Kim, S.J. Moon, H.H. Wang, S. Kim, Y.M. Lee, Mixed matrix membranes with a thermally rearranged polymer and ZIF-8 for hydrogen separation, J. Memb. Sci. 582 (2019) 381–390 10.1016/j.memsci.2019.04.029.
[244] S. Anastasiou, N. Bhoria, J. Pokhrel, K.S. Kumar Reddy, C. Srinivasakannan, K. Wang, G.N. Karanikolos, Metal-organic framework/graphene oxide composite fillers in mixed-matrix membranes for CO_2 separation, Mater. Chem. Phys. 212 (2018) 513–522 10.1016/j.matchemphys.2018.03.064.
[245] K.J. Berean, J.Z. Ou, M. Nour, M.R. Field, M.M.Y.A. Alsaif, Y. Wang, R. Ramanathan, V. Bansal, S. Kentish, C.M. Doherty, A.J. Hill, C. McSweeney, R.B. Kaner, K. Kalantar-zadeh, Enhanced gas permeation through graphene nanocomposites, J. Phys. Chem. C. 119 (2015) 13700–13712 10.1021/acs.jpcc.5b02995.
[246] L. Zhao, C. Cheng, Y.-F. Chen, T. Wang, C.-H. Du, L.-G. Wu, Enhancement on the permeation performance of polyimide mixed matrix membranes by incorporation of graphene oxide with different oxidation degrees, Polym. Adv. Technol. 26 (2015) 330–337 10.1002/pat.3456.
[247] R. Kumar, K. Jayaramulu, T.K. Maji, C.N.R. Rao, Hybrid nanocomposites of ZIF-8 with graphene oxide exhibiting tunable morphology, significant CO_2 uptake and other novel properties, Chem. Commun. 49 (2013) 4947–4949 10.1039/C3CC00136A.
[248] X. Li, L. Ma, H. Zhang, S. Wang, Z. Jiang, R. Guo, H. Wu, X. Cao, J. Yang, B. Wang, Synergistic effect of combining carbon nanotubes and graphene oxide in mixed matrix membranes for efficient CO_2 separation, J. Memb. Sci. 479 (2015) 1–10 10.1016/j.memsci.2015.01.014.
[249] F. Cacho-Bailo, M. Etxeberría-Benavides, O. Karvan, C. Téllez, J. Coronas, Sequential amine functionalization inducing structural transition in an aldehyde-containing zeolitic imidazolate framework: application to gas separation membranes, CrystEngComm 19 (2017) 1545–1554 10.1039/C7CE00086C.